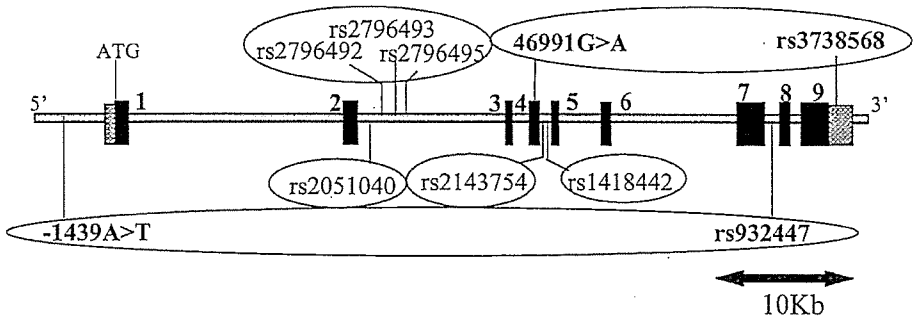

FIG. 1. *PRKAA2* gene structure and haplotype blocks. Structures of *PRKAA2* and SNPs analyzed in this study. Coding and untranslated regions of *PRKAA2* are represented by ■ and ▨, respectively. SNPs identified by sequencing are shown in boldface. Each circle indicates a cluster of SNPs with $r^2 > 0.8$.

consent, and the ethics committee of the University of Tokyo approved this study.

Screening and genotyping of *PRKAA2*. We screened all nine exons, including their exon-intron boundaries, 5′ untranslated region, 3′ untranslated region, and 2,000-bp upstream region of *PRKAA2* in 32 diabetic patients to detect new single nucleotide polymorphisms (SNPs). The primer sequences are available from the authors. SNPs were genotyped by direct sequencing. Sequencing reactions were performed with the BigDye terminator (Applied Biosystems, Foster City, CA) and resolved using an ABI 3700 automated DNA sequencer (Applied Biosystems). The results were integrated using a Sequencher (Gene Codes, Ann Arbor, MI), and individual SNPs were manually genotyped. Ambiguous base identifications were genotyped twice. SNPs were identified based on the sequence reported in GenBank (*PRKAA2*: NT_032977).

Statistical analysis. Genotype or allele associations for each SNP with type 2 diabetes were tested by Fisher's exact test. Homeostasis model assessment (HOMA) of insulin resistance was calculated as described previously for the nondiabetic subjects (11) in the initial samples because insulin therapy or treatment with oral hypoglycemic agents for type 2 diabetes would presum-

TABLE 1
Genotype and allele frequencies for SNPs in *PRKAA2* in case and control samples (initial samples)

				Genotype frequency			Minor allele frequency		
	SNP ID*	Distance from ATG†	Location	Genotype	Case (n = 192)	Control (n = 272)	P value‡	Case/Control	P value§	Odds ratio (95% CI)
	−1439A>T	−1439	Promoter	AA	114 (0.59)	149 (0.55)	0.57	0.22/0.25	0.31	0.85 (0.62–1.16)
				AT	71 (0.37)	110 (0.40)				
				TT	7 (0.04)	13 (0.05)				
SNP1	rs2051040	31695	Intron 2	GG	64 (0.33)	106 (0.39)	0.38	0.41/0.37	0.16	1.21 (0.92–1.58)
				GA	95 (0.50)	129 (0.47)				
				AA	33 (0.17)	37 (0.14)				
	rs2796492	31711	Intron 2	CC	77 (0.40)	85 (0.31)	0.14	0.37/0.42	0.11	0.80 (0.61–1.05)
				CT	87 (0.45)	143 (0.53)				
				TT	28 (0.15)	44 (0.16)				
	rs2796493	31720	Intron 2	GG	76 (0.39)	83 (0.31)	0.12	0.37/0.43	0.07	0.78 (0.60–1.04)
				GA	88 (0.46)	142 (0.52)				
				AA	28 (0.15)	47 (0.17)				
SNP2	rs2796495	31919	Intron 2	GG	75 (0.39)	82 (0.30)	0.13	0.37/0.43	0.09	0.80 (0.60–1.04)
				GA	90 (0.47)	146 (0.54)				
				AA	27 (0.16)	44 (0.16)				
	46991G>A	46991	Exon 4	GG	134 (0.70)	176 (0.65)	0.50	0.17/0.20	0.24	0.81 (0.58–1.14)
				GA	52 (0.27)	85 (0.31)				
				AA	6 (0.03)	11 (0.04)				
SNP3	rs2143754	47801	Intron 4	TT	70 (0.36)	83 (0.30)	0.15	0.40/0.46	0.06	0.77 (0.59–1.01)
				TC	92 (0.48)	128 (0.47)				
				CC	30 (0.16)	61 (0.23)				
SNP4	rs1418442	48077	Intron 4	AA	110 (0.57)	144 (0.53)	0.60	0.24/0.26	0.48	0.89 (0.66–1.21)
				AG	73 (0.38)	116 (0.43)				
				GG	9 (0.05)	12 (0.04)				
SNP5	**rs932447**	59169	Intron 7	AA	113 (0.59)	155 (0.57)	0.81	0.22/0.22	0.83	1.04 (0.76–1.42)
				AG	73 (0.38)	110 (0.40)				
				GG	6 (0.03)	7 (0.03)				
SNP6	**rs3738568**	62531	3′ UTR	TT	153 (0.80)	198 (0.73)	0.22	0.11/0.15	0.12	0.73 (0.49–1.08)
				TC	35 (0.18)	68 (0.25)				
				CC	4 (0.02)	6 (0.02)				

*Newly identified SNPs are shown in boldface. †A of the start codon is counted as 1. P values for ‡genotype frequency and §allele frequency. UTR, untranslated region.

TABLE 2
Haplotype analyses

Haplotype	Initial samples			Replication samples		
SNPs* 1 2 3 4 5 6	Case frequency	Control frequency	Permutation *P* value	Case frequency	Control frequency	Permutation *P* value
n	192	272		657	360	
G G T A A T	0.14	0.18	0.162	0.14	0.17	0.227
A G T A A T	0.38	0.29	**0.009**	0.36	0.32	**0.021**
G A C G G T	0.16	0.19	0.256	0.20	0.19	0.495
G A C A A C	0.08	0.11	0.096	0.12	0.12	0.481

Haplotype	Hiroshima samples			Joint (initial + replication+ Hiroshima) samples		
SNPs* 1 2 3 4 5 6	Case frequency	Control frequency	Permutation *P* value	Case frequency	Control frequency	Permutation *P* value
n	356	192		1,205	824	
G G T A A T	0.15	0.13	0.272	0.15	0.16	0.1175
A G T A A T	0.35	0.26	**0.007**	0.37	0.30	**0.0001**
G A C G G T	0.19	0.16	0.237	0.19	0.18	0.6447
G A C A A C	0.11	0.08	0.232	0.11	0.11	0.6643

*SNP1 is equivalent to rs2051040, SNP2 to rs2796495, SNP3 to rs2143754, SNP4 to rs1418442, SNP5 to rs932447, and SNP6 to rs3738568. The total of the frequencies of the common haplotypes does not reach 1.0 because rare haplotypes with frequencies <0.05 were excluded. *P* values <0.05 are shown in boldface. Given the conservative Bonferroni correction, a *P* value <0.0125 (0.05 divided by four common haplotypes obtained from haplotype frequency estimation) is considered significant in the initial samples. In the replication samples, a *P* value <0.05 is considered significant.

ably alter their insulin levels. A multiple regression analysis was used to test for associations between SNPs and insulin resistance after adjustment for age, sex, and BMI. The statistical analyses were performed using JMP for Windows version 4.00 software (SAS Institute, Cary, NC). *P* values were corrected by Bonferroni adjustment, and a *P* value <0.005 (i.e., 0.05 divided by the total number of SNPs) was considered significant in the initial study. The statistical power was calculated based on a test for differences in proportions of alleles between case and control subjects (described in detail by Ohashi et al. [12]).

Haplotype analysis. To examine the linkage disequilibrium (LD) structure, pairwise LD, D′, and r^2 between SNPs and haplotype frequencies were estimated via the method of maximum likelihood from two-locus genotype data using the E-M algorithm under the assumption of Hardy-Weinberg equilibrium (13). For the estimation of haplotype frequencies, we selected one of the SNPs as a tagging SNP from every set of SNPs with $r^2 > 0.80$. All haplotypes were jointly tested for association with disease status by performing a $2 \times n\chi^2$ test of independence in a permutation procedure, where n indicates the number of haplotypes with a frequency >0. Individual haplotypes were also tested for association with disease status with a $2 \times 2\chi^2$ test of independence in a permutation procedure. In the permutation procedure, to account for the variability introduced by the haplotype frequency estimation, significance was assessed by permuting case and control status and recalculating the test statistic 1,000 times for each of the sample sets and 10,000 times for the combined sample set. The above calculations were performed with SNPAlyze V3.2 Pro software (Dynacom, Yokohama, Japan).

RESULTS AND DISCUSSION

We identified four SNPs by screening *PRKAA2*, two SNPs of which were also reported in the public database (Fig. 1). Adding 6 more SNPs available in the JSNP (Japanese Single Nucleotide Polymorphisms) database (available at http://snp.ims.u-tokyo.ac.jp/), a total of 10 SNPs were genotyped in the initial samples. All the polymorphisms were in Hardy-Weinberg equilibrium and had a minor allele frequency >5%. None of the SNPs was associated with type 2 diabetes (Table 1 and online appendix Tables 1–3 [available at http://diabetes.diabetesjournals.org]). Neither the difference in genotype frequency nor that in allele frequency had any significant influence on susceptibility to type 2 diabetes.

The LD pattern and the D′ and r^2 values of the 192 diabetic patients providing the initial sample are shown in Fig. 2. The six groups of SNPs with r^2 values >0.8 and each of the tagging SNPs (SNPs 1–6) are shown in Figs. 1 and 2. All the haplotypes with frequencies >5% for the entire sample are shown in Table 2. A general $2 \times n$ test for independence revealed a significant difference ($P = 0.009$) in haplotype frequencies with a minor (*A*) allele for rs2051040 and a major allele for all the other SNPs (AGTAAT) between case and control samples. Other common haplotypes were not associated with type 2 diabetes. These results were confirmed in a larger replication sample with 657 diabetic patients and 360 nondiabetic subjects. The haplotype with the *A* (minor) allele for rs2051040 and a major allele for the other five SNPs was associated with type 2 diabetes ($P = 0.021$) (Table 2). Even a genetically homogenous population, such as that of Iceland, has been reported to show substantial divergence in allele frequencies among geographical areas (14). Therefore, we further confirmed the association between the haplotype AGTAAT and type 2 diabetes in a third panel ($P = 0.007$) (Table 2), for which we enrolled both 356 type 2 diabetic and *192* nondiabetic subjects from the same area of Japan (Hiroshima) to exclude the possibility that the associations with the haplotype were falsely obtained as a result of population stratification among subjects enrolled from different areas of Japan.

A joint analysis of the whole sample revealed a significant association between haplotype AGTAAT and type 2 diabetes ($P = 0.0001$) (Table 2). The total of the frequencies of the common hapolotypes is <1.0 because rare haplotypes with frequencies <0.05 were excluded. The complete set of all estimated haplotypes for the case and control subjects is shown in online appendix Table 4.

We next investigated whether the polymorphisms in *PRKAA2* were associated with insulin resistance, as assessed by HOMA of insulin resistance. The association was compared between subjects with and without the minor allele. Among the 10 SNPs investigated, only

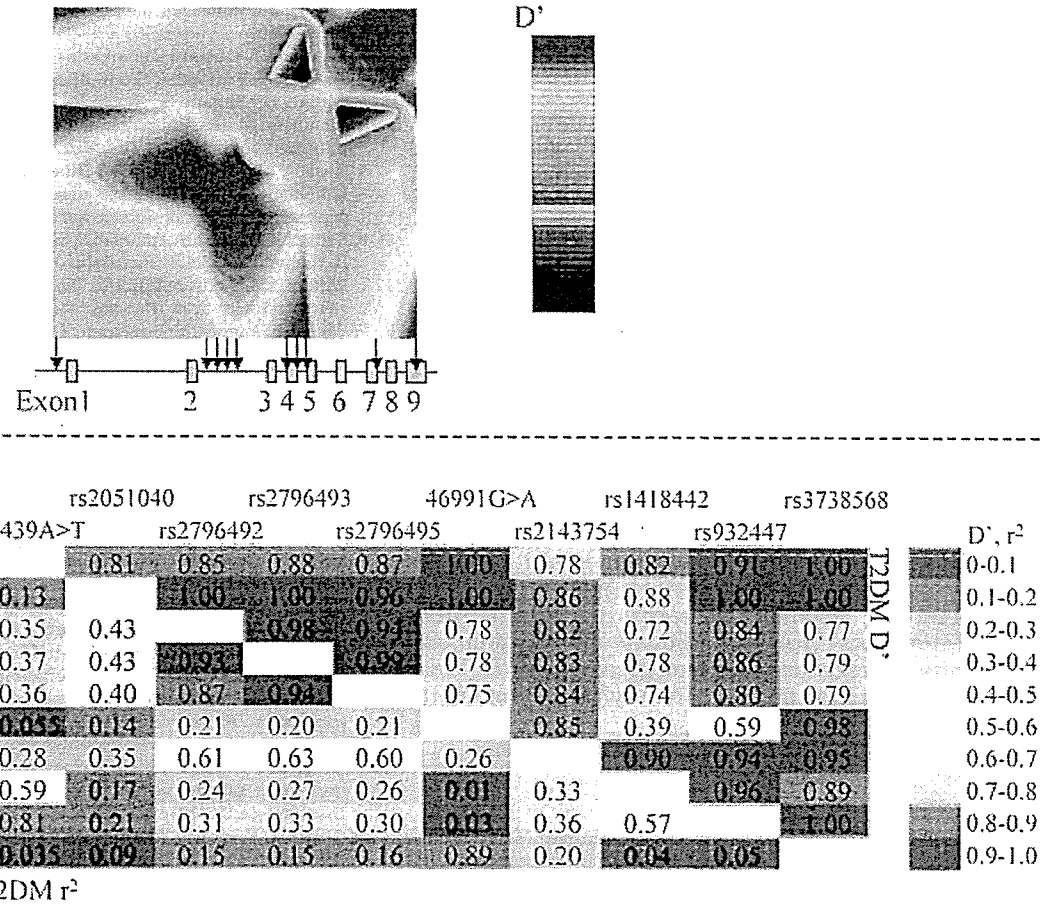

FIG. 2. Pairwise LD between SNPs. The *lower left* and *upper right* triangles indicate pairwise LD and r^2 and D' values, respectively, in 192 type 2 diabetic (T2DM) patients. Underlined SNPs are the tagging SNPs that represent all of the tested SNPs based on $r^2 > 0.8$.

rs2051040 was associated with insulin resistance. Subjects with the *A* (minor) allele for rs2051040 had a higher HOMA of insulin resistance than those without it (*AA/AG* vs. *GG* 1.95 ± 0.08 vs. 1.49 ± 0.10, regression coefficient = 0.18, $P = 0.002$). This finding was also confirmed in the joint replication samples (*AA/AG* vs. *GG* 1.83 ± 0.07 vs. 1.59 ± 0.09, regression coefficient = 0.099, $P = 0.037$). No other SNPs were associated with insulin resistance or any other diabetes-related quantitative traits, such as age, sex, BMI, fasting glucose, fasting insulin, HbA_{1c}, and HOMA-β.

PRKAA2 is a good candidate for the susceptibility gene to insulin resistance and type 2 diabetes. We therefore focused on *PRKAA2* and genotyped 10 SNPs spanning from the promoter region to the 3′ untranslated region. Even though alleles with an odds ratio of 1.2–1.3 could be detected with 80% power for the total sample for allele frequencies of 0.2 and 0.4, which correspond to the commonly observed allele frequencies in this study, we were unable to find associations between any single polymorphisms and type 2 diabetes. However, one common haplotype with the *A* (minor) allele for rs2051040 and a major allele for all the other SNPs was associated with type 2 diabetes. To jointly test all common haplotypes for associations with disease status, we also used PHASE version 2.1, performing a case-control permutation test with the default setting. In agreement with the haplotype analysis using SNPAlyze, haplotype analysis using PHASE software revealed a significant difference ($P = 0.01$) in haplotype frequencies between case and control subjects (data not shown). Likewise, SNPAlyze also revealed a significant difference (global $P = 0.004$) in a permutation test for differences in haplotype frequencies between case and control subjects. We therefore conclude that there is a significant difference in haplotype frequencies between case and control subjects and that this difference may be attributable to the haplotype AGTAAT, i.e., the haplotype with a minor (*A*) allele for rs2051040 and a major allele for all the other SNPs.

This intronic SNP rs2051040 alone was not associated with type 2 diabetes, but it was significantly associated with insulin resistance ($P = 0.002$), consistent with the known function of AMPK. The association was still significant even when the conservative Bonferroni adjustment was taken into account. Subjects with the *A* allele for rs2051040 had more marked insulin resistance, and a haplotype containing the *A* allele for rs2051040 was observed more frequently in case compared with control subjects. The initial results were further confirmed in the joint replication samples.

The risk haplotype frequency is quite close to the frequency of rs2051040 in the case subjects, for example 0.38 and 0.41 in the initial sample, but quite different, 0.29 and 0.37, respectively, in the control subjects. The A allele of rs2051040 is present on a rare haplotype, AGCAAT, whose frequency is higher in the control than in the case subjects, and the presence of this haplotype appears to be responsible for the discrepancy between the A allele of

rs2051040 and risk haplotype frequencies in the case and control subjects (online appendix Table 4).

We note two possible reasons why the association between rs2051040 and type 2 diabetes is evident in haplotypic, but not individual SNP, association analyses. One possibility is that an unidentified SNP, which is in LD with this risk haplotype but is in weaker LD with rs2051040, is the SNP actually causing type 2 diabetes. The other possibility is that rs2051040 and another SNP, contained in this risk haplotype, function in a coordinate manner to increase the risk of type 2 diabetes. The HapMap shows additional SNPs in the Chinese/Japanese sample between exon 1 and 2 of PRKAA2, where SNP finding was scarce in our study. An intronic SNP that is associated with type 2 diabetes in Japanese subjects may lie in this region. Further research to identify either the true causative SNP or as-yet-unidentified SNPs functioning in a coordinate manner with rs2051040 is needed.

ACKNOWLEDGMENTS

This work was supported by a Grant-in-Aid from the Pharmaceuticals and Medical Devices Agency (to T.K.); a Grant-in-Aid for Scientific Research on Priority Areas "Applied Genomics" from the Ministry of Education, Culture, Sports, Science and Technology of Japan (to T.K.); and a Grant-in-Aid for the 21st Century COE Program (to R.N.).

We thank Ms. Y. Okada for technical assistance.

REFERENCES

1. Mu J, Brozinick JT, Valladares O, Bucan M, Birnbaum MJ: A role for AMP-activated protein kinase in contraction- and hypoxia-regulated glucose transport in skeletal muscle. *Molec Cell* 7:1085–1094, 2001
2. Zhou G, Myers R, Li Y, Chen Y, Shen X, Fenyk-Melody J, Wu M, Ventre J, Doebber T, Fujii N, Musi N, Hirshman MF, Goodyear LJ, Moller DE: Role of AMP-activated protein kinase in mechanism of metformin action. *J Clin Invest* 108:1167–1174, 2001
3. Minokoshi Y, Kim YB, Peroni OD, Fryer LGD, Müller C, Carling D, Kahn BB: Leptin stimulates fatty-acid oxidation by activating AMP-activated protein kinase. *Nature* 415:339–343, 2002
4. Yamauchi T, Kamon J, Minokoshi Y, Ito Y, Waki H, Uchida S, Yamashita S, Noda M, Kita S, Ueki K, Eto K, Akanuma Y, Froguel P, Foufelle F, Ferre P, Carling D, Kimura S, Nagai R, Kahn BB, Kadowaki T: Adiponectin stimulates glucose utilization and fatty-acid oxidation by activating AMP-activated protein kinase. *Nat Med* 8:1288–1295, 2002
5. Musi N, Hayashi T, Fujii N, Hirshman MF, Witters LA, Goodyear LJ: AMP-activated protein kinase activity and glucose uptake in rat skeletal muscle. *Am J Physiol Endocrinol Metab* 280:E677–E684, 2001
6. Foretz M, Ancellin N, Andreelli F, Saintillan Y, Grondin P, Kahn A, Thorens B, Vaulont S, Viollet B: Short-term overexpression of a constitutively active form of AMP-activated protein kinase in the liver leads to mild hypoglycemia and fatty liver. *Diabetes* 54:1331–1339, 2005
7. Viollet B, Andreelli F, Jorgensen SB, Perrin C, Flamez D, Mu J, Wojtaszewski JF, Schuit FC, Birnbaum M, Richter E, Burcelin R, Vaulont S: Physiological role of AMP-activated protein kinase (AMPK): insights from knockout mouse models. *Biochem Soc Trans* 31:216–219, 2003
8. Beri RK. Marley AE, See CG, Sopwith WF, Aguan K, Carling D, Scott J, Carey F: Molecular cloning, expression and chromosomal localisation of human AMP-activated protein kinase. *FEBS Lett* 356:117–121, 1994
9. Mori Y, Otabe S, Dina C, Yasuda K, Populaire C, Lecoeur C, Vatin V, Durand E, Hara K, Okada T, Tobe K, Boutin P, Kadowaki T, Froguel P: Genome-wide search for type 2 diabetes in Japanese affected sibpairs confirms susceptibility genes on 3q, 15q, and 20q and identifies two new candidate loci on 7p and 11p. *Diabetes* 51:1247–1255, 2002
10. Hara K, Boutin P, Mori Y Tobe K, Dina C, Yasuda K, Yamauchi T, Otabe S, Okada T, Eto K, Kadowaki H, Hagura R, Akanuma Y, Yazaki Y, Nagai R, Taniyama M, Matsubara K, Yoda M, Nakano Y, Tomita M, Kimura S, Ito C, Froguel P, Kadowaki T: Genetic variation in the gene encoding adiponectin is associated with an increased risk of type 2 diabetes in the Japanese population. *Diabetes* 51:536–540, 2002
11. Matthews DR, Hosker JP, Rudenski AS, Naylor BA, Treacher DF, Turner RC: Homeostasis model assessment: insulin resistance and beta-cell function from fasting plasma glucose and insulin concentrations in man. *Diabetologia* 28:412–419, 1985
12. Ohashi J, Maruya E, Tokunaga K, Saji H: Power of association test for detecting minor histocompability gene causing graft-versus-host disease following bone marrow transplantation. *J Hum Genet* 48:502–507, 2003
13. Excoffier L, Slatkin M: Maximum-liklifood estimation of molecular haplotype frequencies in a dipolid population. *Mol Biol Evol* 5:921–927, 1995
14. Helgason A, Yngvadottir B, Hrafnkelsson B, Gulcher J, Stefansson K: An Icelandic example of the impact of population structure on association studies. *Nat Genet* 37:90–95, 2005

Original Article

Peroxisome Proliferator–Activated Receptor (PPAR)α Activation Increases Adiponectin Receptors and Reduces Obesity-Related Inflammation in Adipose Tissue

Comparison of Activation of PPARα, PPARγ, and Their Combination

Atsushi Tsuchida,[1] Toshimasa Yamauchi,[1,2] Sato Takekawa,[1] Yusuke Hada,[1] Yusuke Ito,[1] Toshiyuki Maki,[1] and Takashi Kadowaki[1,2,3]

We examined the effects of activation of peroxisome proliferator–activated receptor (PPAR)α, PPARγ, and both of them in combination in obese diabetic KKAy mice and investigated the mechanisms by which they improve insulin sensitivity. PPARα activation by its agonist, Wy-14,643, as well as PPARγ activation by its agonist, rosiglitazone, markedly improved insulin sensitivity. Interestingly, dual activation of PPARα and -γ by a combination of Wy-14,643 and rosiglitazone showed increased efficacy. Adipocyte size in Wy-14,643–treated KKAy mice was much smaller than that of vehicle- or rosiglitazone-treated mice, suggesting that activation of PPARα prevents adipocyte hypertrophy. Moreover, Wy-14,643 treatment reduced inflammation and the expression of macrophage-specific genes in white adipose tissue (WAT). Importantly, Wy-14,643 treatment upregulated expression of the adiponectin receptor (AdipoR)-1 and AdipoR2 in WAT, which was decreased in WAT of KKAy mice compared with that in nondiabetic control mice. Furthermore, Wy-14,643 directly increased expression of AdipoRs and decreased monocyte chemoattractant protein-1 expression in adipocytes and macrophages. Rosiglitazone increased serum adiponectin concentrations and the ratio of high molecular weight multimers of adiponectin to total adiponectin. A combination of rosiglitazone and Wy-14,643 increased both serum adiponectin concentrations and AdipoR expression in WAT. These data suggest that PPARα activation prevents inflammation in WAT and that dual activation of PPARα and -γ enhances the action of adiponectin by increasing both adiponectin and AdipoRs, which can result in the amelioration of obesity-induced insulin resistance. *Diabetes* 54:3358–3370, 2005

Peroxisome proliferator–activated receptor (PPAR)α and -γ are ligand-activated transcription factors and members of the nuclear hormone receptor superfamily that regulate the metabolism of glucose and lipids (1–6). PPARγ is one of the key regulators of glucose homeostasis, and the molecular mechanisms concerning how the activation of PPARγ improves insulin sensitivity have been well investigated. Activation of PPARγ by agonists such as thiazolidinediones (TZDs) stimulates lipid storage in adipocytes, thereby reducing lipotoxicity in liver and skeletal muscle (7). In addition, PPARγ activation increases small adipocytes, thereby increasing the insulin-sensitizing hormone adiponectin and reducing resistin and tumor necrosis factor (TNF)-α, which induce insulin resistance (8,9). However, PPARγ agonists are associated with body weight gain, which is a clinical drawback for treatment of type 2 diabetic patients. In contrast, it has been previously reported that PPARα agonists prevent the development of obesity-induced insulin resistance in rodents without inducing body weight gain (10–12); however, the mechanisms by which the activation of PPARα improves insulin resistance are not fully understood.

Recently, it has been reported that chronic inflammation in white adipose tissue (WAT) by macrophage infiltration may cause whole-body insulin resistance in obese diabetic animals (13,14). Activated macrophages that infiltrate into WAT secrete cytokines that can impair adipocyte insulin sensitivity. Adipocytes stimulated by proinflammatory cytokines secrete chemokines that can contribute to macrophage infiltration. This vicious cycle impairs adipocyte insulin signaling and may eventually cause systemic insulin resistance (13,14). Moreover, inflammatory markers such as C-reactive protein are associated with insulin resistance, adiposity, and type 2 diabetes in human subjects (15–17). Therefore, it has become important to investigate the mechanisms of insulin-sensitizing drugs by focusing on the regulation of inflammation.

In this study, we examined the effects of activation of

From the [1]Department of Metabolic Diseases, Graduate School of Medicine, University of Tokyo, Tokyo, Japan; the [2]Core Research for Evolutional Science and Technology of Japan Science and Technology Agency, Kawaguchi, Japan; and the [3]National Institute of Health and Nutrition, Tokyo, Japan.

Address correspondence and reprint requests to Takashi Kadowaki, MD, PhD, Department of Metabolic Diseases, Graduate School of Medicine, University of Tokyo, 7-3-1 Hongo, Bunkyo-ku, Tokyo 113-8655, Japan. E-mail: kadowaki-3im@h.u-tokyo.ac.jp.

Received for publication 26 May 2005 and accepted in revised form 1 September 2005.

A.T. and T.Y. contributed equally to this work.

AdipoR, adiponectin receptor; BAT, brown adipose tissue; DMEMH, Dulbecco's modified high-glucose Eagle's medium; HMW, high molecular weight; MCP, monocyte chemotactic protein; PDK4, pyruvate dehydrogenase kinase isozyme 4; PPAR, peroxisome proliferator–activated receptor; TNF, tumor necrosis factor; TZD, thiazolidinedione; UCP, uncoupling protein; WAT, white adipose tissue.

PPARα, PPARγ, and both in combination in obese diabetic KKAy mice, and we investigated the mechanisms by which they improve insulin resistance, especially in WAT. The results indicate that PPARα activation prevents infiltration of macrophages into WAT, thereby ameliorating inflammation of WAT, which can result in improvement of obesity-induced insulin resistance. We also demonstrate that dual activation of PPARα and -γ enhances the action of adiponectin in WAT by increasing both adiponectin and the expression of its receptors.

RESEARCH DESIGN AND METHODS

Rosiglitazone was synthesized as described elsewhere (18). Wy-14,643 was purchased from Biomol Research Laboratories (Plymouth Meeting, PA). All materials were obtained from sources described previously (8,9,19).

We purchased 6-week-old male KKAy mice and age-matched KK mice from Nippon CLEA (Shizuoka, Japan). KKAy mice are an obese diabetic model in which the Ay mutation is introduced onto a KK strain background. Therefore, we used KK mice as nondiabetic controls. Mice were housed singly and maintained on a 12-h light/dark cycle. The high-fat diet consisted of 32% (wt/wt) fat as described previously (20). KKAy mice were given the high-fat diet, and KK mice were given normal chow. High-fat feeding was begun 1 week before rosiglitazone or Wy-14,643 administration. Rosiglitazone or Wy-14,643 was given as a 0.01 and 0.05% food admixture, respectively. These doses were chosen because they have been shown to be effective therapeutic doses in diabetic mice (21–24). The same amount of food was given to the pair-fed group of KKAy mice as that fed to the Wy-14,643–treated group of KKAy mice. The animal care procedures and methods were approved by the animal care committee of the University of Tokyo.

Blood sample assays and in vivo glucose homeostasis. The glucose tolerance and insulin tolerance tests were carried out according to previously described methods (9). Plasma glucose, serum free fatty acid, and triglyceride levels were determined by a glucose test, nonesterified fatty acid-C test, and triglyceride L-type (Wako Pure Chemical Industries, Osaka, Japan), respectively. Plasma insulin was measured by an insulin immunoassay (Shibayagi, Gunma, Japan). Plasma leptin and adiponectin levels were determined by a Quintikine M kit (R&D Systems, Minneapolis, MN) and mouse adiponectin immunoassay kit (Otsuka Pharmaceutical, Tokushima, Japan), respectively (20). Detection of multimer species of adiponectin was conducted as described previously (25). In brief, 0.7 μl of serum was subjected to 2–15% SDS-PAGE under nonreducing and non–heat-denaturing conditions. Adiponectin was detected using anti–globular domain antiserum obtained by immunizing rabbits with mouse recombinant adiponectin globular domain produced in *Escherichia coli* (25).

Histological analysis of adipose tissue. Epididymal adipose tissue was removed from each animal, fixed in 10% formaldehyde/PBS, and maintained at 4°C until use. Fixed specimens were dehydrated, embedded in tissue-freezing medium (Tissue-Tek OCT compound; Miles, Elkhart, IN), and frozen in dry ice and acetone. WAT was cut into 10-μm sections, and the sections were mounted on silanized slides. The adipose tissue was stained with hematoxylin and eosin (7) or anti-mouse F4/80 antibody (Serotec, Raleigh, NC) (13).

Quantitative analysis by real-time PCR. Total RNA was prepared from cells or tissues with TRIzol (Invitrogen, Carlsbad, CA) according to the manufacturer's instructions. A real-time PCR method was used to quantify the AdipoRs mRNAs (19). The primer sets and the probes for mAdipoR1 and -R2 were as follows: the forward primer for mAdipoR1 was acgttggagagtcatcccg tat, the reverse primer ctctgtgtggatgcggaagat, and the probe cctgctacatggcca cagaccacct; the forward primer for mAdipoR2 was tcccaggaagatgaagggtttat, the reverse primer ttccattcgttcgatagcatga, and the probe atgtccccgctcctacagg ccc. For quantification of the other genes, we used a set of predesigned primers and a probe for each gene (Assay on Demand; Applied Biosystems, Foster City, CA). The relative amount of each transcript was normalized to the amount of β-actin transcript in the same cDNA (19).

Isolation of adipocytes and stromal-vascular cells. Isolation of adipocytes and stromal-vascular cells from adipose tissues were performed as described previously, with slight modification (13). Epididymal adipose tissues were isolated from mice and were minced into fine pieces. Minced tissues were incubated in Dulbecco's modified Eagle's medium supplemented with 5 mg/ml collagenase (Sigma, St. Louis, MO) and 2.5% BSA (Sigma) at 37°C for 40–45 min. Digested samples were passed through a sterile 250-μm nylon mesh and centrifuged. The pellet cells and the floating cells were washed twice with PBS and collected as the stromal-vascular cells and adipocytes, respectively. In the experiments of direct action of PPAR agonists on primary adipocytes and stromal-vascular cells, 1×10^5 isolated adipocytes were seeded onto 24-well plates in Dulbecco's modified high-glucose Eagle's medium (DMEMH) supplemented with 20% charcoal-treated FCS, and 1×10^5 isolated stromal-vascular cells were seeded onto 96-well plates in DMEMH supplemented with 20% charcoal-treated FCS and mouse granulocyte colony-stimulating factor (R&D Systems). Then, the cells were incubated with 3 μmol/l Wy-14,643 or 0.3 μmol/l rosiglitazone for 24 h and then harvested to isolate total RNA.

Studies with 3T3-L1 adipocytes and peritoneal macrophages. Mouse 3T3-L1 cells were grown in DMEMH supplemented with 10% FCS. Induction of adipogenic differentiation was carried out according to a method described previously (8). By day 8, 3T3-L1 adipocytes were incubated with 30 μmol/l Wy-14,643 or 0.3 μmol/l rosiglitazone in DMEMH supplemented with 1% BSA for 18 h, and then 1 ng/ml TNF-α was added. The cells were harvested 6 h after TNF-α addition to isolate total RNA. Peritoneal macrophages were isolated as previously described (26). In brief, macrophages were isolated 4 days after intraperitoneal injection of 3 ml thioglycolate medium (Sigma) to male C57BL/6j mice. Then, 1,000,000 cells were plated onto 24-well plates in RPMI-1640/10% FBS (vol/vol) and incubated for 4 h. Then, the macrophages were incubated with 30 μmol/l Wy-14,643, 100 μmol/l fenofibrate, or 0.3 μmol/l rosiglitazone in the presence of 0.1 μg/ml lipopolysaccharide for 24 h and then harvested to isolate total RNA. The concentrations of the compounds in the in vitro cell culture experiments were chosen according to previous studies, and they were comparable to those to which PPARα in animal tissues were exposed in previous in vivo studies (8,10–12,27,28).

Statistical analysis. Data are the means ± SE. Student's *t* test was used for statistical comparison. $P < 0.05$ was considered statistically significant.

RESULTS

A PPARα agonist improves insulin resistance in KKAy mice, and a combination of a PPARα agonist and a PPARγ agonist enhances the antidiabetic effects of the PPARγ agonist. To examine the antidiabetic effects of a dual activation of PPARα and -γ in comparison with a single activation of each alone, we treated obese diabetic KKAy mice with a PPARγ agonist, rosiglitazone, a PPARα agonist, Wy-14,643, or a combination of the two for 8 weeks. We then examined the glucose and lipid metabolism and insulin sensitivity of these mice. Because it has been previously reported that PPARα agonists reduce food intake in rodents (28), pair-fed control mice were given daily the same amount of food as that consumed by Wy-14,643–treated mice (Fig. 1*F*). As shown in Fig. 1, Wy-14,643 treatment significantly ameliorated hyperglycemia (Fig. 1*A*), hyperinsulinemia (Fig. 1*B*), and hyperlipidemia (Fig. 1*C* and *D*) compared with ad libitum–fed vehicle-treated KKAy mice. Because these effects of Wy-14,643 were significant even in comparison with pair-fed mice (Fig. 1*A–D*), it is likely that Wy-14,643 actually exerted its antidiabetic effects via a mechanism other than decreased food intake. Blood glucose (Fig. 1*A*) and plasma insulin levels (Fig. 1*B*) in the rosiglitazone-treated mice were significantly lower than those in the ad libitum–fed vehicle-treated mice. However, the serum lipid levels of the rosiglitazone-treated mice were significantly higher than those of the Wy-14,643–treated mice (Fig. 1*C* and *D*). Interestingly, a combination of rosiglitazone and Wy-14,643 completely normalized the hyperglycemia (Fig. 1*A*), hyperinsulinemia (Fig. 1*B*), and hyperlipidemia (Fig. 1*C* and *D*) observed in KKAy mice, and, in particular, the blood glucose (Fig. 1*A*) and lipid levels (Fig. 1*C* and *D*) in the combined rosiglitazone- and Wy-14,643–treated mice were significantly lower than those in the rosiglitazone-treated mice. Furthermore, serum lipid levels in the combined rosiglitazone- and Wy-14,643–treated mice were significantly lower than those in the Wy-14,643–treated mice (Fig. 1*C* and *D*). Although body weight was slightly lower in the Wy-14,643–treated mice ($P = 0.093$) than in the pair-fed vehicle-treated mice, the difference was not statistically significant (Fig. 1*E*).

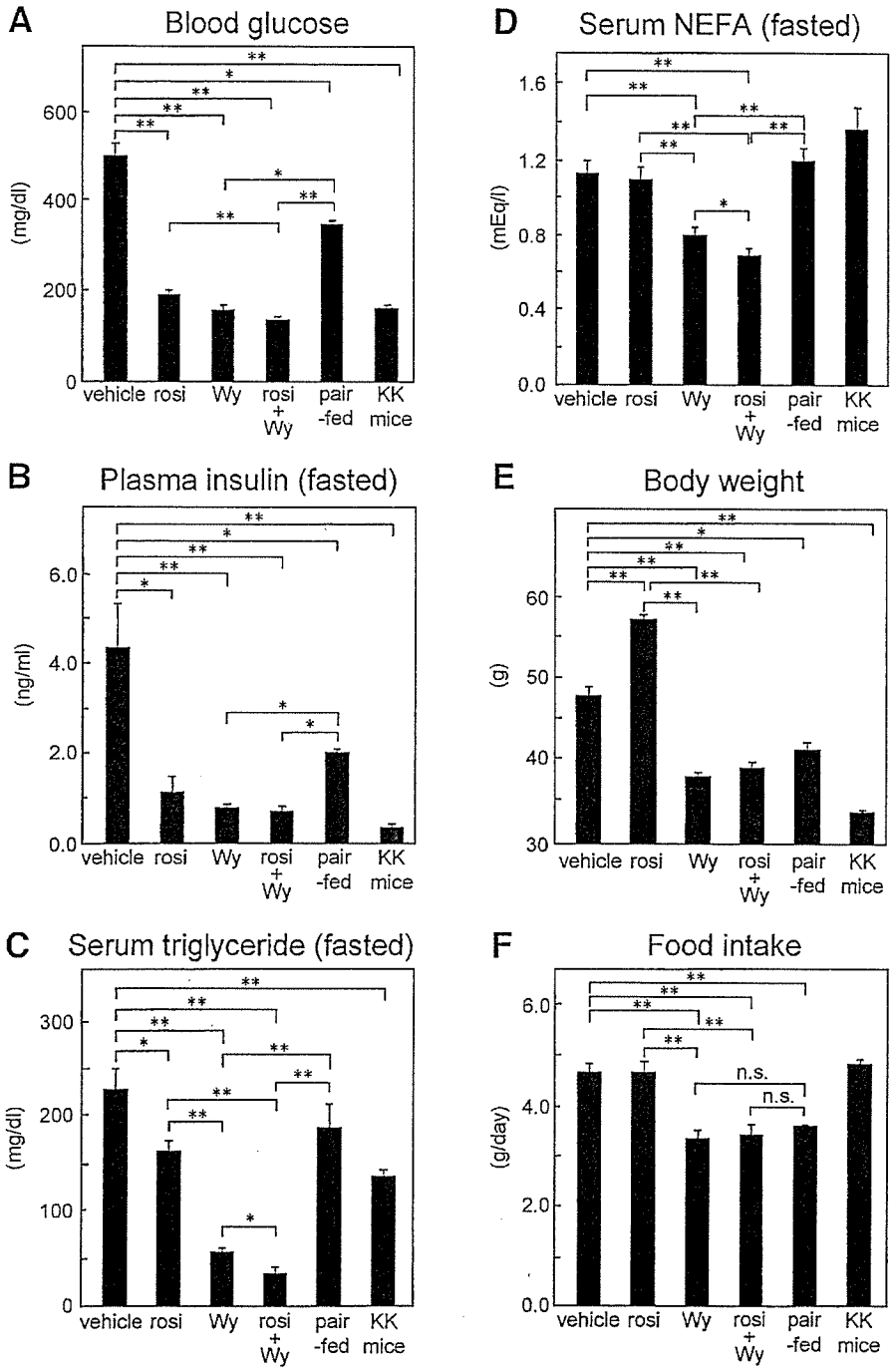

FIG. 1. Effects of rosiglitazone, Wy-14,643, or both rosiglitazone and Wy-14,643 treatment for 8 weeks on serum parameters and body weight in KKAy mice. Panels show blood glucose (*A*), fasting plasma insulin (*B*), fasting serum triglycerides (*C*), fasting NEFA (*D*), body weight (*E*), and food intake (*F*) of male KKAy mice treated with 0.01% rosiglitazone (rosi), 0.05% Wy-14,643 (Wy), or both 0.01% rosiglitazone and 0.05% Wy-14,643 (rosi+Wy) as food admixture for 8 weeks while on the high-fat diet. The same amount of food was given to the pair-fed group as to mice treated with Wy-14,643. Age-matched wild-type KK mice given normal chow were used as normal controls. Fasting parameters were measured after a 24-h fast. Each bar represents the means ± SE (n = 4 for pair-fed group, n = 6 for other groups). *P < 0.05; **P < 0.01. NEFA, nonesterified fatty acid; n.s., not significant.

We next examined the effects of PPARα and -γ activation on the improvement of insulin resistance in more detail, using a glucose tolerance test and insulin tolerance test. Blood glucose levels during both tests in Wy-14,643–treated mice were significantly lower than those in pair-fed vehicle-treated mice (Fig. 2*A* and *C*), suggesting that Wy-14,643 treatment ameliorated insulin resistance. Again, the combination of rosiglitazone and Wy-14,643 ameliorated insulin resistance more effectively than rosiglitazone or Wy-14,643 alone (Fig. 2*B* and *C*).

Adipocyte hypertrophy is prevented by a PPARα agonist. It has been reported that PPARα agonists prevent high-fat diet–induced obesity (10). Thus, we measured epididymal and subcutaneous WAT and intrascapular brown adipose tissue (BAT) weights. Wy-14,643 decreased both WAT and BAT weights compared with pair-fed mice (Fig. 3*A–C*), suggesting that PPARα activation prevents obesity. The combination of rosiglitazone and Wy-14,643 decreased only epididymal WAT weights compared with pair-fed mice (Fig. 3*A*). In contrast, rosiglitazone increased subcutaneous WAT and BAT weights compared with vehicle (Fig. 3*B* and *C*).

We have previously shown that PPARγ activation by its agonist or a moderate reduction of PPARγ activity prevents adipocyte hypertrophy, which results in an improvement in insulin resistance (7). We next attempted to clarify

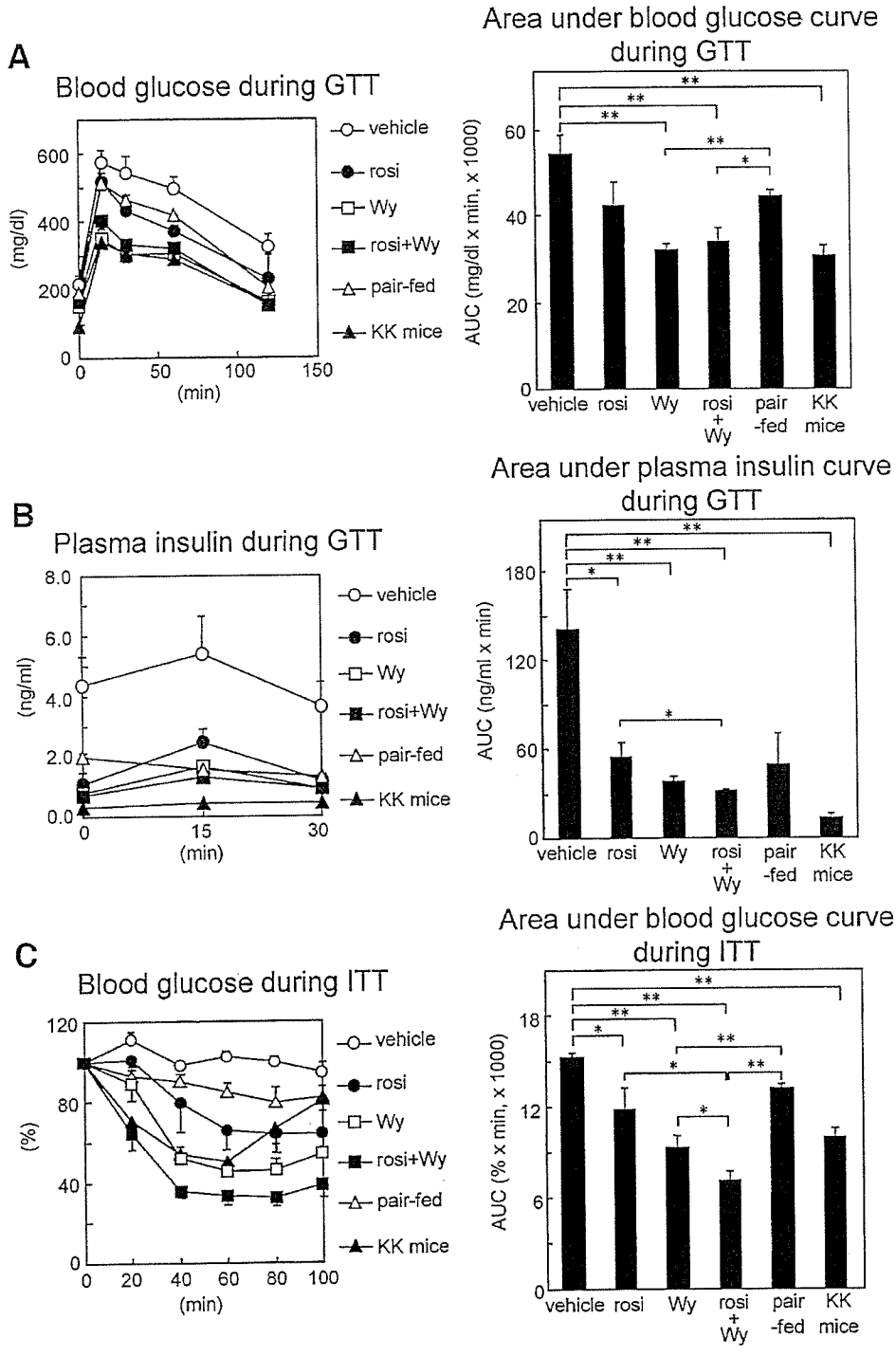

FIG. 2. Effects of rosiglitazone, Wy-14,643, or both rosiglitazone and Wy-14,643 treatment for 8 weeks on glucose tolerance and insulin sensitivity in KKAy mice. We measured blood glucose (*A*) and plasma insulin (*B*) during oral glucose tolerance tests (GTTs) and blood glucose during insulin tolerance tests (ITTs) (*C*) of male KKAy mice treated with 0.01% rosiglitazone (rosi), 0.05% Wy-14,643 (Wy), or both 0.01% rosiglitazone and 0.05% Wy-14,643 (rosi+Wy) as a food admixture for 8 weeks while on the high-fat diet. The same amount of food was given to the pair-fed group as to mice treated with Wy-14,643. Age-matched wild-type KK mice given normal chow were used as normal controls. Oral glucose tolerance tests were performed by oral gavage of 0.75 g/kg body wt glucose after 24 h fasting followed by blood sampling at the indicated time. Insulin tolerance tests were performed by 1.5 units/kg body wt i.p. insulin followed by blood sampling at the indicated time. Each bar represents the means ± SE (n = 4 for pair-fed group, n = 6 for other groups). ○, vehicle; ●, rosiglitazone; □, Wy-14,643; ■, both rosiglitazone and Wy-14,643; △, pair-fed; ▲, KK mice. $^*P < 0.05$; $^{**}P < 0.01$.

whether adipocyte hypertrophy and increased fat pad weight are suppressed by PPARα activation. The size of the adipose cells in epididymal WAT was increased in KKAy mice (Fig. 4*A*, *upper left*) compared with the wild-type control KK mice (Fig. 4*A*, *lower right*). Very interestingly, the size of the adipose cells in epididymal WAT from Wy-14,643–treated mice (Fig. 4*A*, *upper right*) was dramatically decreased compared with that from pair-fed mice (Fig. 4*A*, *lower middle*) and was comparable to that in the wild-type control KK mice (Fig. 4*A*, *lower right*). Although rosiglitazone treatment (Fig. 4*A*, *upper middle*) increased the ratio of small adipocytes in epididymal WAT compared with vehicle treatment (Fig. 4*A*, *upper left*), the changes were moderate compared with Wy-14,643 treatment (Fig. 4*A*, *upper right*). The size of the adipose cells in epididymal WAT from mice treated with a combination of rosiglitazone and Wy-14,643 (Fig. 4*A*, *lower left*) was also smaller than that from pair-fed mice (Fig. 4*A*, *lower middle*). The size of the adipose cells in subcutaneous WAT from Wy-14,643–treated mice was also decreased compared with that from pair-fed mice (Fig. 4*B*). There were small nucleated cells and macrophage-specific antigen F4/80–

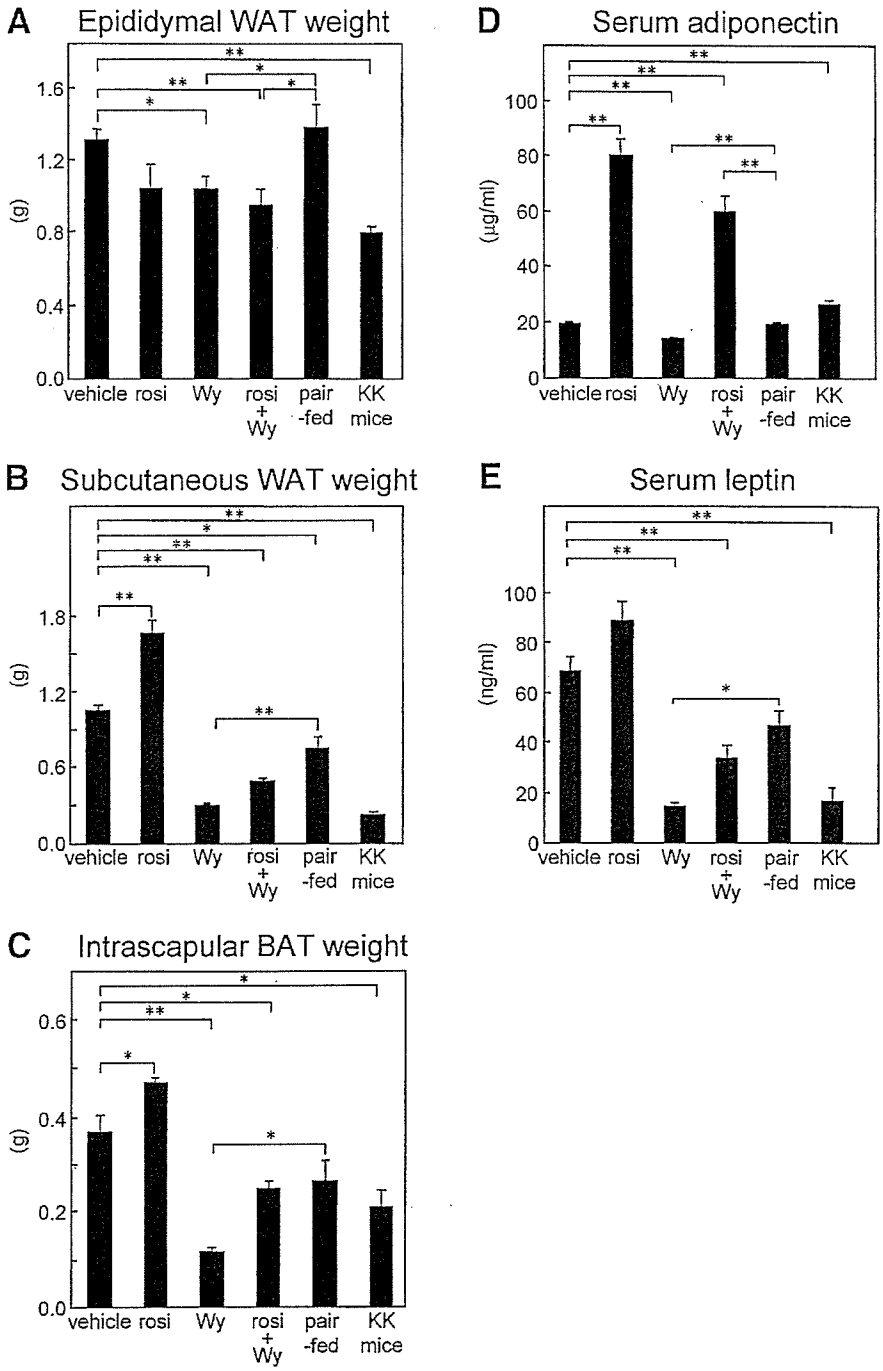

FIG. 3. Effects of rosiglitazone, Wy-14,643, or both rosiglitazone and Wy-14,643 treatment for 8 weeks on fat pad weight and serum adipokines in KKAy mice. Panels show epididymal WAT weight (*A*), subcutaneous WAT weight (*B*), intrascapular BAT weight (*C*), serum adiponectin levels (*D*), and serum leptin levels (*E*) of male KKAy mice treated with 0.01% rosiglitazone (rosi), 0.05% Wy-14,643 (Wy), or both 0.01% rosiglitazone and 0.05% Wy-14,643 (rosi+Wy) as a food admixture for 8 weeks while on the high-fat diet. The same amount of food was given to the pair-fed group as to mice treated with Wy-14,643. Age-matched wild-type KK mice given normal chow were used as normal controls. Each bar represents the means ± SE ($n = 4$ for pair-fed group, $n = 6$ for other groups). *$P < 0.05$; **$P < 0.01$.

expressing cells in the interstitial spaces between adipocytes in WAT of vehicle-treated KKAy mice (Fig. 4*C*). In contrast, there were almost no such cells in the WAT of Wy-14,643–treated mice (Fig. 4*C*), suggesting that macrophage infiltration to WAT may be suppressed by Wy-14,643 treatment, whereas the effect of rosiglitazone treatment seemed to be faint. We obtained similar results with BAT (Fig. 4*D*), except that the size of the adipocytes in BAT from rosiglitazone-treated mice (Fig. 4*D*, *upper middle*) was larger than that in vehicle-treated mice (Fig. 4*D*, *upper left*).

We next studied whether the levels of expression of molecules secreted from WAT that regulate insulin sensitivity were changed by PPARα activation. As reported previously (9), serum adiponectin levels in rosiglitazone-treated mice were higher by fourfold than those in vehicle-treated mice (Fig. 3*D*). In contrast, serum adiponectin levels in Wy-14,643–treated mice were slightly lower than those in pair-fed mice, suggesting that the improvement in insulin resistance by Wy-14,643 was not caused by increased gene expression or secretion of adiponectin (Fig. 3*D*). The combination of rosiglitazone and Wy-14,643 increased serum adiponectin levels approximately threefold above the vehicle (Fig. 3*D*). Serum leptin levels in KKAy mice were increased by overexpression of agouti compared with those in wild-type KK mice (Fig. 3*E*). Wy-14,643

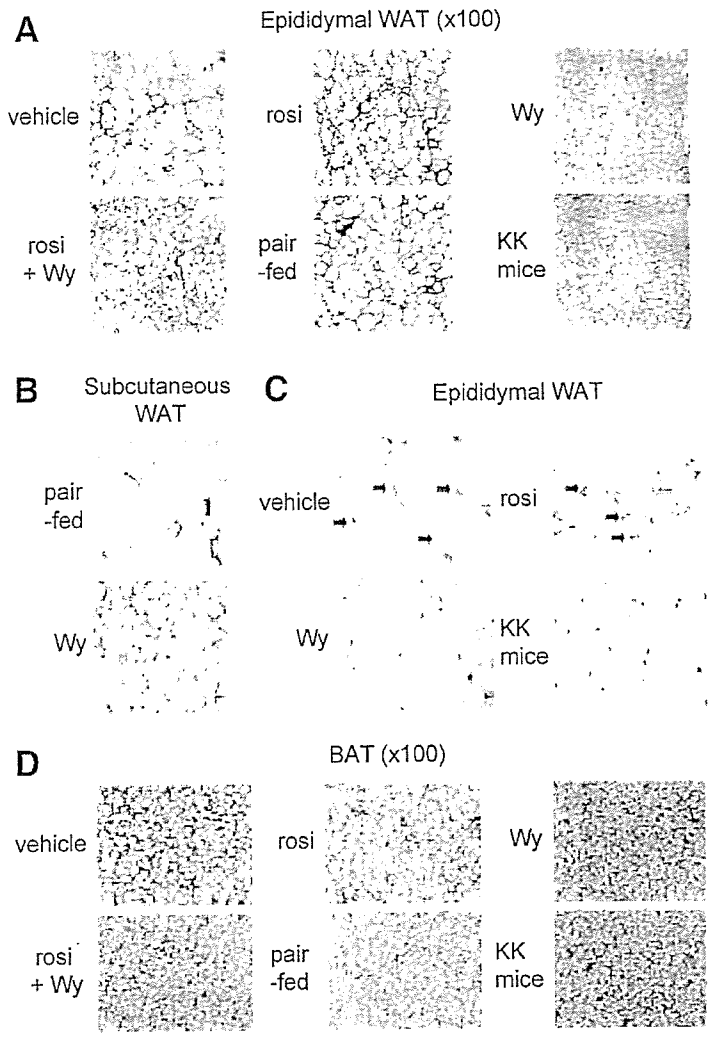

FIG. 4. Histological analyses of WAT and BAT from KKAy mice treated with rosiglitazone, Wy-14,643, or both rosiglitazone and Wy-14,643 for 8 weeks. Panels show the sections of epididymal WAT (*A* and *C*), subcutaneous WAT (*B*), and BAT (*D*), which were stained with hematoxylin and eosin (*A*, *B*, and *D*) or anti-F4/80 antibody (*C*), of male KKAy mice were treated with 0.01% rosiglitazone (rosi), 0.05% Wy-14,643 (Wy), or both 0.01% rosiglitazone and 0.05% Wy-14,643 (rosi+Wy) as a food admixture for 8 weeks while on the high-fat diet. The same amount of food was given to the pair-fed group as to mice treated with Wy-14,643. Age-matched wild-type KK mice given normal chow were used as normal controls. Arrows indicate F4/80-expressing cells.

treatment decreased the serum leptin levels to levels comparable to wild-type KK mice (Fig. 3*E*). Although rosiglitazone treatment slightly ($P = 0.057$) increased serum leptin levels, combined rosiglitazone and Wy-14,643 treatment decreased them compared with vehicle (Fig. 3*E*).

A PPARα agonist increases molecules involved in fatty acid combustion in liver and BAT. PPARα is abundantly expressed in liver and BAT in rodents, and PPARα activation induces fatty acid combustion (29,30). Thus, we examined the gene expression of molecules involved in fatty acid oxidation and lipolysis, using quantitative PCR analyses. As shown in Fig. 5*B* and *C*, the expression of uncoupling protein (UCP)-1 and β3-adrenergic receptor in BAT were decreased in vehicle-treated KKAy mice compared with wild-type KK mice, consistent with the adipocyte hypertrophy observed in KKAy mice (Fig. 5*C*). Wy-14,643 treatment increased the expression of UCP2 in liver (Fig. 5*A*) and the expression of UCP1 and β3-adrenergic receptor in BAT (Fig. 5*B* and *C*). In contrast, rosiglitazone treatment decreased the expression of UCP1 and β3-adrenergic receptor in BAT compared with vehicle (Fig. 5*B* and *C*). Combined treatment with rosiglitazone and Wy-14,643 increased the expression of UCP2 (Fig. 5*A*), but it did not affect the expression of UCP1 and β3-adrenergic receptor in BAT compared with vehicle (Fig. 5*B* and *C*). Taken together, these findings suggest that the induction of molecules involved in fatty acid combustion in liver and BAT is, at least in part, responsible for the prevention of adipocyte hypertrophy by PPARα activation.

A PPARα agonist suppresses inflammation in WAT. Recently, it was proposed that obesity-related insulin resistance may be a chronic inflammatory disease initiated in adipose tissue (13,14). Although it has been reported that rosiglitazone suppressed the expression of inflammation genes in WAT of obese diabetic *ob/ob* mice (14), the effects of PPARα agonists on inflammation in WAT have not yet been studied in detail. We studied whether Wy-14,643 suppressed the expression of inflammatory genes in WAT. As shown in Fig. 5*D–F*, the expression of TNF-α, monocyte chemotactic protein (MCP)-1, and macrophage antigen-1 in WAT of vehicle-treated KKAy mice were significantly increased compared with wild-type KK mice, suggesting that the accumulation of macrophages and inflammatory responses were induced in WAT of KKAy mice. Interestingly, Wy-14,643 treatment suppressed the increased expression of TNF-α, MCP-1, and macrophage antigen-1 in WAT compared with vehicle (Fig. 5*D–F*), which was consistent with the suppression of macrophage infiltration into WAT by Wy-14,643 treatment (Fig. 4*C*). Rosiglitazone treatment partially suppressed the expression of MCP-1 in WAT (Fig. 5*F*), but it did not affect the expression of TNF-α and macrophage antigen-1 compared

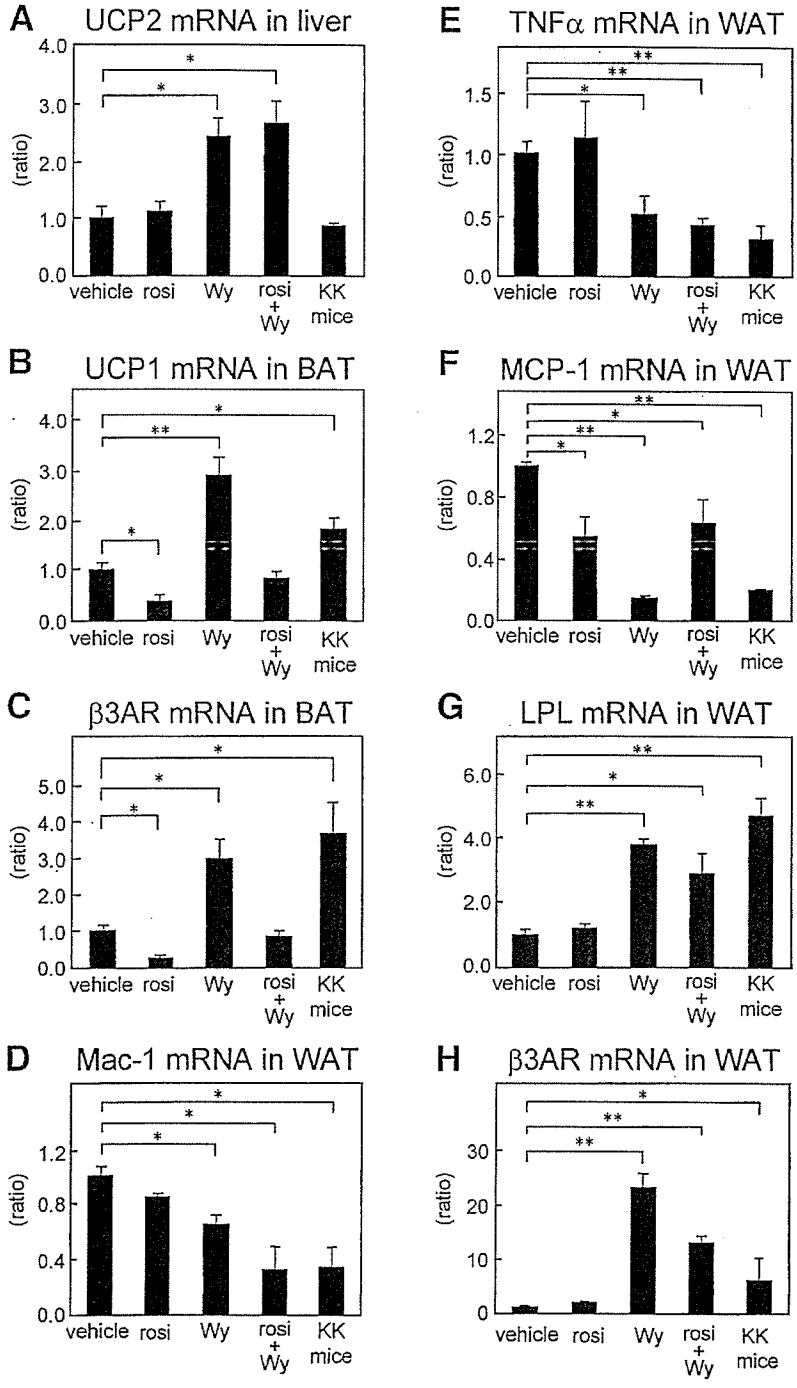

FIG. 5. Effects of rosiglitazone, Wy-14,643, or both rosiglitazone and Wy-14,643 treatment for 8 weeks on expression of molecules involving fatty acid combustion and inflammation in liver, BAT, and WAT from KKAy mice. Panels show amounts of mRNAs of UCP2 in liver (*A*); UCP1 (*B*) and β3-adrenergic receptor (*C*) in BAT; and macrophage antigen (Mac)-1 (*D*), TNF-α (*E*), MCP-1 (*F*), lipoprotein lipase (*G*), and β3-adrenergic receptor (β3AR) (*H*) in epididymal WAT of male KKAy mice treated with 0.01% rosiglitazone (rosi), 0.05% Wy-14,643 (Wy), or both 0.01% rosiglitazone and 0.05% Wy-14,643 (rosi+Wy) as food admixture for 8 weeks while on the high-fat diet. Age-matched wild-type KK mice given normal chow were used as normal controls. Amounts of the mRNAs of molecules indicated above were quantified by a real-time PCR method as described in RESEARCH DESIGN AND METHODS. The relative amount of each transcript was normalized to the amount of β-actin transcript in the same cDNA. The results are expressed as the ratio of the value of vehicle-treated KKAy mice. Each bar represents the means ± SE (n = 3). *P < 0.05; **P < 0.01.

with vehicle (Fig. 5*D* and *E*). Combined rosiglitazone and Wy-14,643 treatment, as well as Wy-14,643 treatment, suppressed the expression of these genes compared with vehicle (Fig. 5*D–F*).

It has been reported that MCP-1 decreased the expression of genes involved in adipocyte function and attenuated insulin sensitivity in cultured adipocytes (31). Thus, we examined the effects of PPARα activation on the expression of lipoprotein lipase and β3-adrenergic receptor in WAT. The expression of lipoprotein lipase and β3-adrenergic receptor were decreased in WAT of vehicle-treated KKAy mice compared with wild-type KK mice (Fig. 5*G* and *H*). Wy-14,643 treatment increased the expression of lipoprotein lipase and β3-adrenergic receptor in WAT, whereas rosiglitazone treatment showed no effect (Fig. 5*G* and *H*). Taken together, these data suggest that Wy-14,643 suppressed inflammation in WAT and normalized gene expression, which were dysregulated by obesity-associated adipocyte hypertrophy and inflammation.

A PPARα agonist increases the expression of adiponectin receptors (AdipoRs) in WAT, whereas a PPARγ agonist increases the ratio of high molecular weight multimers of adiponectin to total adiponectin. We previously reported that AdipoR1 and -2 are downregulated in WAT, BAT, and skeletal muscles in obese diabetic *ob/ob* mice, which are correlated with decreased adiponec-

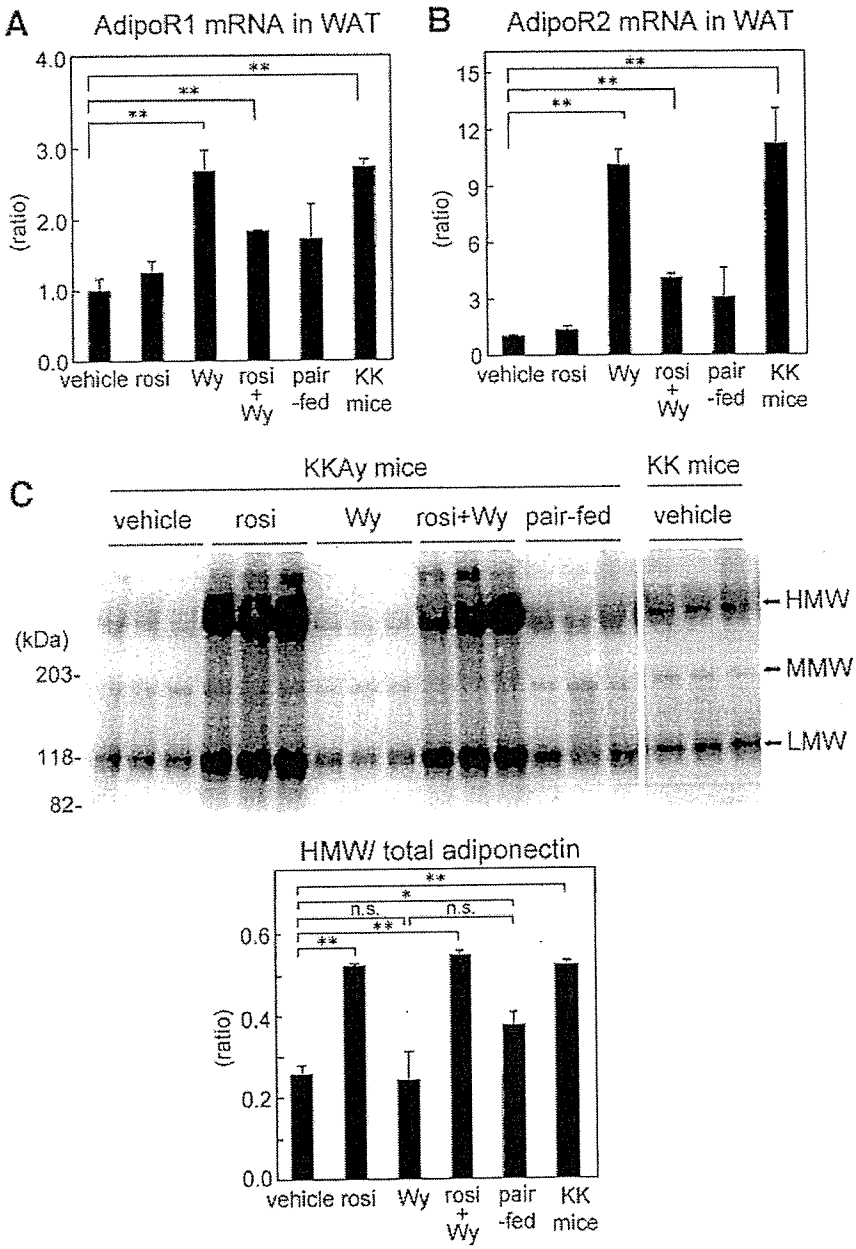

FIG. 6. Effects of rosiglitazone, Wy-14,643, or both rosiglitazone and Wy-14,643 treatment for 8 weeks on expression of AdipoR1/R2 in WAT and multimer forms of serum adiponectin in KKAy mice. Panels show amounts of mRNAs of AdipoR1 (*A*) and AdipoR2 (*B*) in epididymal WAT of male KKAy mice treated with 0.01% rosiglitazone (rosi), 0.05% Wy-14,643 (Wy), or both 0.01% rosiglitazone and 0.05% Wy-14,643 (rosi+Wy) as food admixture for 8 weeks while on the high-fat diet. The same amount of food was given to the pair-fed group as to mice treated with Wy-14,643. Age-matched wild-type KK mice given normal chow were used as normal controls. Amounts of the mRNAs of AdipoR1/R2 were quantified by a real-time PCR method as described in RESEARCH DESIGN AND METHODS. The relative amount of each transcript was normalized to the amount of β-actin transcript in the same cDNA. The results are expressed as the ratio of the value of vehicle-treated KKAy mice. Serum of KKAy mice treated with compounds mentioned above was subjected to SDS-PAGE under nonreducing, non–heat-denaturing conditions, and multimer forms of adiponectin were detected, using anti-adiponectin antibody (*C*). *D*: The quantitative results of upper panels. Each bar represents the means ± SE (n = 3). *P < 0.05; **P < 0.01. LMW, low molecular weight; n.s., not significant.

tin sensitivity (32). As shown in Fig. 6*A* and *B*, the expression of AdipoR1 and -2 was decreased in WAT of vehicle-treated KKAy mice compared with wild-type KK mice. Wy-14,643 treatment almost completely reversed the decrease in AdipoR1 and -2 expression in KKAy mice (Fig. 6*A* and *B*). In contrast, the expression levels of AdipoR1 and -2 were not affected by rosiglitazone treatment, whereas combined rosiglitazone and Wy-14,643 treatment partially reversed the decrease in these genes (Fig. 6*A* and *B*). We also obtained similar results in BAT (data not shown).

Adiponectin is known to form characteristic multimers (33,34). It was recently reported that the increase in the ratio of the high molecular weight (HMW) form to total adiponectin is correlated with an improvement in insulin sensitivity by TZD treatment (35). Here, we studied whether a PPARα agonist affects the forms of serum adiponectin. As shown in Fig. 6*C*, the ratio of HMW to total adiponectin was decreased in vehicle-treated KKAy mice compared with wild-type KK mice. The restriction of food intake by pair-fed mice partially restored the decrease in the ratio of HMW to total adiponectin in KKAy mice (Fig. 6*C*). Wy-14,643 treatment did not affect the ratio of HMW to total adiponectin, whereas rosiglitazone treatment dramatically increased total adiponectin and the ratio of HMW to total adiponectin (Fig. 6*C*). Treatment with a combination of rosiglitazone and Wy-14,643 showed results similar to rosiglitazone treatment (Fig. 6*C*).

A PPARα agonist directly increased AdipoR expression and suppressed MCP-1 expression. There is a possibility that long-term treatment with Wy-14,643 indirectly increased the gene expression in the WAT of KKAy mice via an improvement in insulin resistance or some other mechanism. Therefore, we examined the effects of short-term treatment with Wy-14,643 on the expression of AdipoR1, AdipoR2, MCP-1, and β3-adrenergic receptor in WAT of KKAy mice. As shown in Fig. 7*A–D*, treatment with

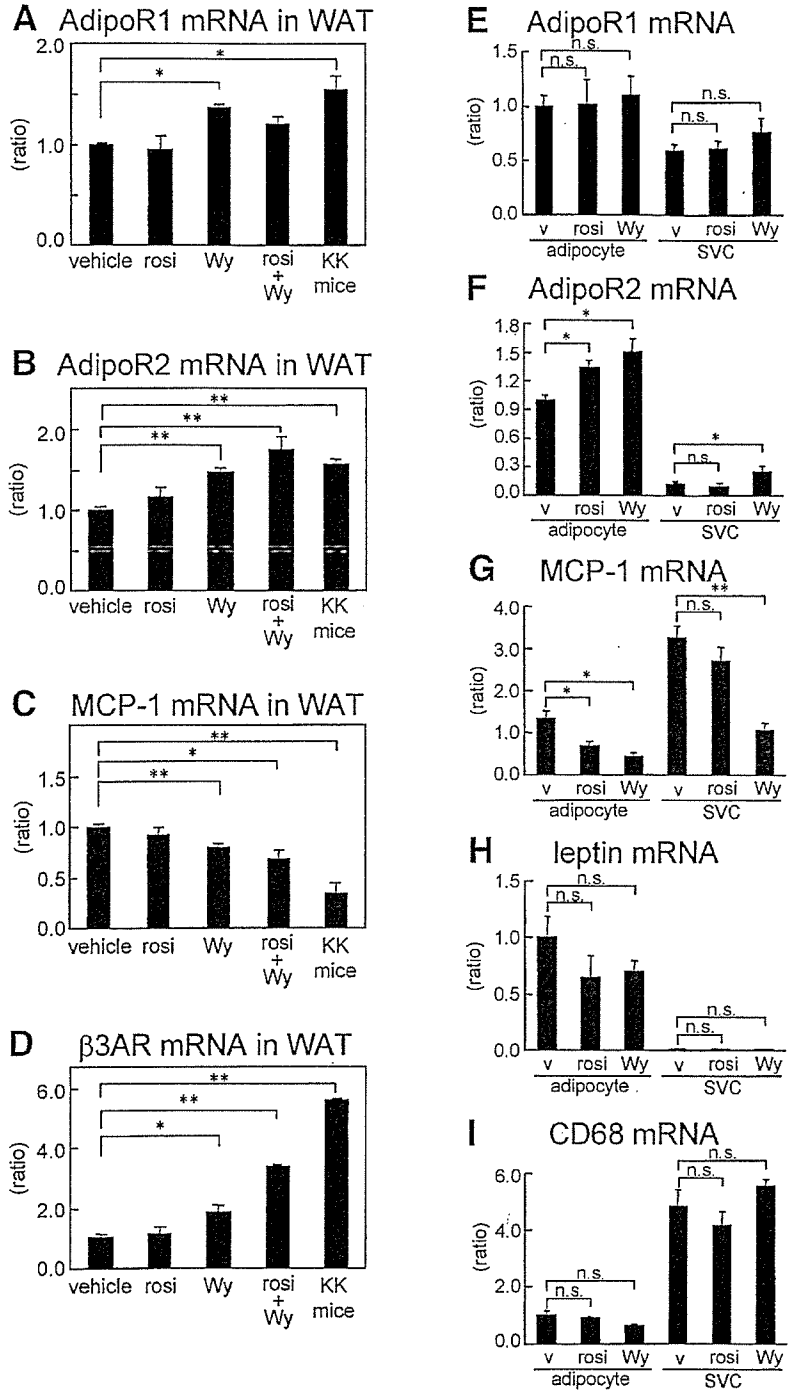

FIG. 7. Effects of rosiglitazone, Wy-14,643, or both rosiglitazone and Wy-14,643 treatment for 3 days on expression of AdipoR1/R2, MCP-1, and β3-adrenergic receptor in WAT of KKAy mice and action of Wy-14,643 on expression of AdipoR1/R2 and MCP-1 in adipocyte (adi) and stromal-vascular cell subfractions of WAT. Panels show amounts of mRNAs of AdipoR1 (*A*), AdipoR2 (*B*), MCP-1 (*C*), and β3-adrenergic receptor (β3AR) (*D*) in epididymal WAT of male KKAy mice treated with 0.01% rosiglitazone (rosi), 0.05% Wy-14,643 (Wy), or both 0.01% rosiglitazone and 0.05% Wy-14,643 (rosi+Wy) as a food admixture for 3 days while on the high-fat diet. Age-matched wild-type KK mice given normal chow were used as normal controls. Amounts of mRNAs of AdipoR1 (*E*), AdipoR2 (*F*), and MCP-1 (*G*) from adipocyte and stromal-vascular cell subfractions of WAT of KKAy mice treated with 0.01% rosiglitazone or 0.05% Wy-14,643 for 3 days while on the high-fat diet. Amounts of the mRNAs of molecules indicated above were quantified by a real-time PCR method as described in RESEARCH DESIGN AND METHODS. The relative amount of each transcript was normalized to the amount of β-actin transcript in the same cDNA. The results are expressed as the ratio of the value of vehicle (v). Each bar represents the means ± SE (n = 3). *P < 0.05; **P < 0.01. n.s., not significant; SVC, stromal-vascular cell.

Wy-14,643 for 3 days increased the expression of AdipoR1, AdipoR2, and β3-adrenergic receptor and decreased the expression of MCP-1 in WAT of KKAy mice. We obtained similar results with the combined treatment of rosiglitazone and Wy-14,643 (Fig. 7*A–D*).

WAT of obese diabetic mice is thought to consist of adipocytes and stromal vascular cells, such as infiltrated macrophages (13,14). We next tried to determine in which cell type the observed effects occur by analyzing the adipocyte and stromal-vascular cell subfractions of adipose tissue separately. As shown in Fig. 7*F* and *G*, treatment with Wy-14,643 for 3 days increased the expression of AdipoR2 and decreased the expression of MCP-1 in both adipocytes and stromal-vascular cells, whereas rosiglitazone treatment showed similar effects only in adipocytes. The expression pattern of leptin and CD68, markers of adipocytes and stromal-vascular cells, respectively, confirmed that the fractionation was performed properly (Fig. 7*H* and *I*).

We next examined the expression of PPARα in the adipose tissue fractions, cultured 3T3-L1 adipocytes, and peritoneal macrophages to determine whether the effects of Wy-14,643 on adipocytes and macrophages were mediated by PPARα. PPARα expression was observed in both the adipose fraction and 3T3-L1 adipocytes as well as in skeletal muscle of KKAy mice (Fig. 8*A*), whereas PPARα

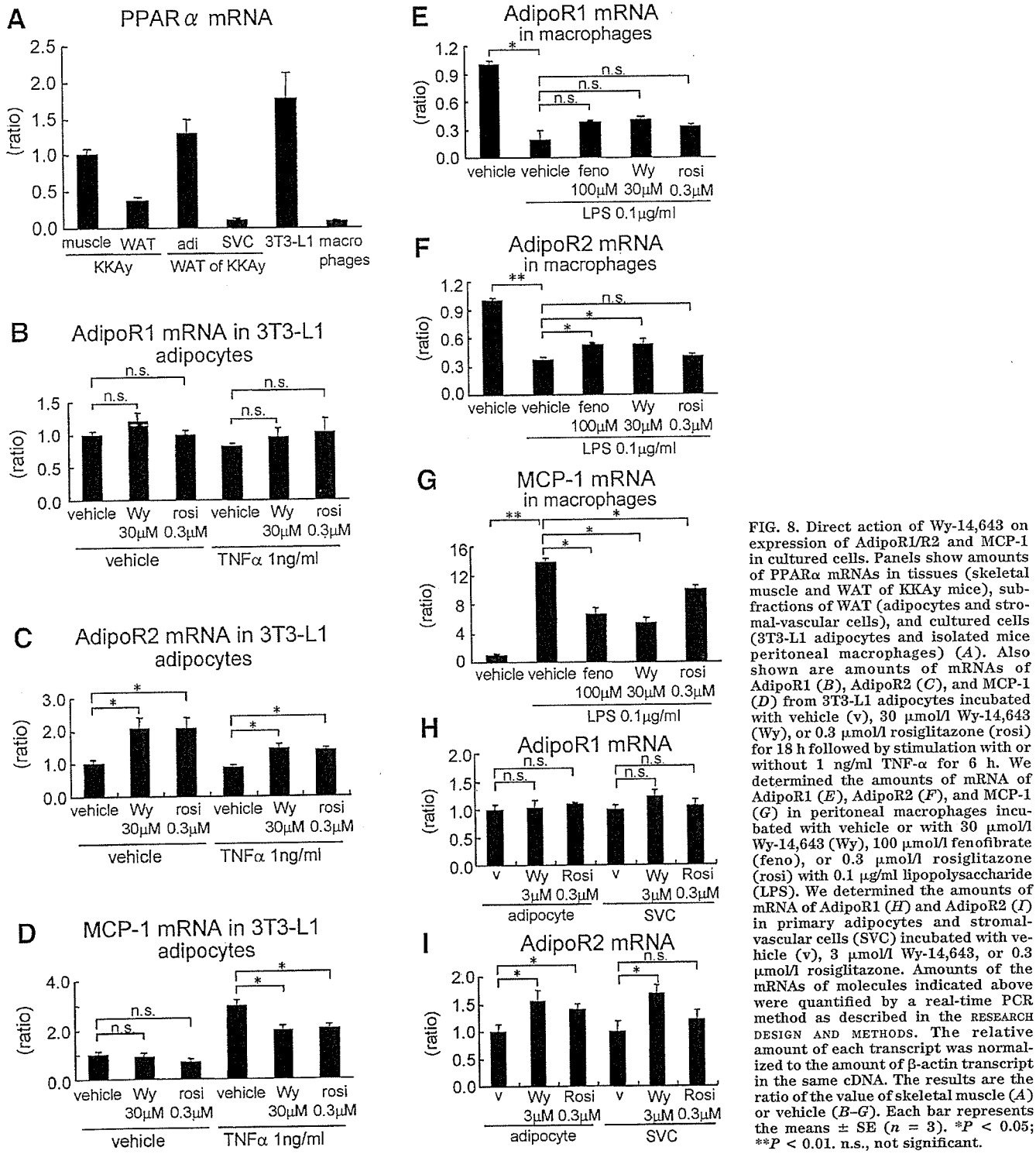

FIG. 8. Direct action of Wy-14,643 on expression of AdipoR1/R2 and MCP-1 in cultured cells. Panels show amounts of PPARα mRNAs in tissues (skeletal muscle and WAT of KKAy mice), subfractions of WAT (adipocytes and stromal-vascular cells), and cultured cells (3T3-L1 adipocytes and isolated mice peritoneal macrophages) (*A*). Also shown are amounts of mRNAs of AdipoR1 (*B*), AdipoR2 (*C*), and MCP-1 (*D*) from 3T3-L1 adipocytes incubated with vehicle (v), 30 μmol/l Wy-14,643 (Wy), or 0.3 μmol/l rosiglitazone (rosi) for 18 h followed by stimulation with or without 1 ng/ml TNF-α for 6 h. We determined the amounts of mRNA of AdipoR1 (*E*), AdipoR2 (*F*), and MCP-1 (*G*) in peritoneal macrophages incubated with vehicle or with 30 μmol/l Wy-14,643 (Wy), 100 μmol/l fenofibrate (feno), or 0.3 μmol/l rosiglitazone (rosi) with 0.1 μg/ml lipopolysaccharide (LPS). We determined the amounts of mRNA of AdipoR1 (*H*) and AdipoR2 (*I*) in primary adipocytes and stromal-vascular cells (SVC) incubated with vehicle (v), 3 μmol/l Wy-14,643, or 0.3 μmol/l rosiglitazone. Amounts of the mRNAs of molecules indicated above were quantified by a real-time PCR method as described in the RESEARCH DESIGN AND METHODS. The relative amount of each transcript was normalized to the amount of β-actin transcript in the same cDNA. The results are the ratio of the value of skeletal muscle (*A*) or vehicle (*B–G*). Each bar represents the means ± SE (n = 3). $^*P < 0.05$; $^{**}P < 0.01$. n.s., not significant.

expression levels in stromal-vascular cells and peritoneal macrophages were much lower than those in skeletal muscle of KKAy mice (Fig. 8*A*). We further examined the direct action of Wy-14,643 on gene expression in cultured adipocytes or macrophages. A 24-h treatment with 30 μmol/l Wy-14,643 significantly increased AdipoR2 expression in 3T3-L1 adipocytes (Fig. 8*C*), whereas AdipoR1 expression was not significantly increased (Fig. 8*B*). Wy-14,643 treatment suppressed the expression of MCP-1, which was increased by 1 ng/ml TNF-α stimulation in 3T3-L1 adipocytes (Fig. 8*D*). Fenofibrate treatment (100 μmol/l) also increased AdipoR2 expression by 25% compared with vehicle in 3T3-L1 adipocytes (data not shown). Wy-14,643 treatment as well as fenofibrate treatment suppressed the increase in MCP-1 expression caused by 0.1 μg/ml lipopolysaccharide treatment and slightly but significantly increased AdipoR2 expression in peritoneal macrophages (Fig. 8*F* and *G*). Rosiglitazone treatment increased

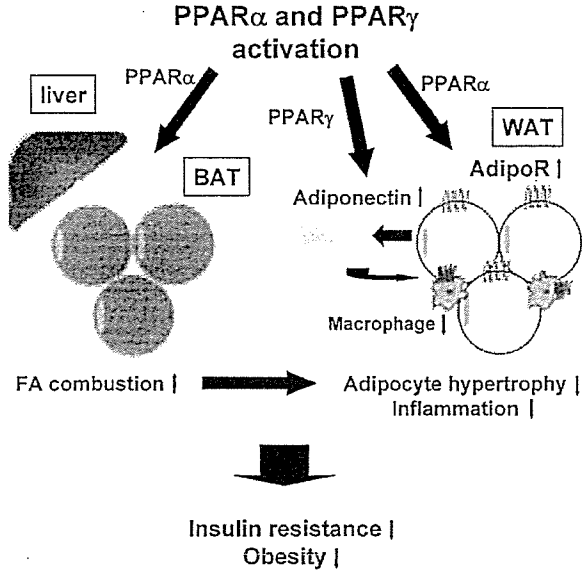

FIG. 9. Proposed mechanisms for improvement of insulin resistance by PPARα and -γ. Activation of PPARα, at least in part, directly suppresses inflammation and adipocyte hypertrophy in WAT in addition to stimulating fatty acid (FA) combustion in liver and BAT. Dual activation of PPARα and -γ enhances the action of adiponectin by increasing AdipoR expression and the ratio of HMW to total adiponectin leading to enhancement of action of adiponectin.

AdipoR2 expression only in 3T3-L1 adipocytes (Fig. 8*C*) and suppressed MCP-1 expression in both adipocytes and macrophages (Fig. 8*D* and *G*), whereas the effect of Wy-14,643 treatment on macrophages was more potent than that of rosiglitazone treatment (Fig. 8*G*). Furthermore, we examined the direct action of the lower concentration of Wy-14,643 on gene expression in primary cultured adipocytes or stromal-vascular cells. A 24-h treatment with 3 μmol/l Wy-14,643 significantly increased AdipoR2 expression in adipocytes and stromal-vascular cells (Fig. 8*I*), whereas AdipoR1 expression was not significantly increased (Fig. 8*H*). These data suggest that Wy-14,643 directly increased AdipoR2 expression in adipocytes and suppressed MCP-1 expression in both adipocytes and macrophages.

DISCUSSION

Recent studies have revealed that adipose tissue plays a key role in regulating whole-body glucose metabolism (13,14,36). In this study, we attempted to clarify the mechanisms by which activation of PPARα and/or PPARγ ameliorates insulin resistance, focusing on adipose tissue. We demonstrate here that activation of PPARα prevented adipocyte hypertrophy, at least in part, through mechanisms other than decreased food intake. As shown in Fig. 9, one possible and conventional mechanism for this effect is an increase in systemic energy expenditure by the induction of molecules involved in fatty acid combustion, such as UCPs in liver and BAT (Fig. 5*A–C*) (27,37,38). We propose that there is also another pathway in which the activation of PPARα in WAT normalizes adipocyte function associated with an increase in β3-adrenergic receptor, which is expressed in WAT and BAT and has been shown to play important roles in lipolysis and thermogenesis (39,40). WAT has not been considered as a main target tissue of PPARα agonist so far (29,30). PPARα mRNA was, however, actually detected by real-time PCR analysis in the adipocyte subfraction of WAT and 3T3-L1 adipocytes (although the expression levels were much lower in adipocytes compared with liver), as well as in skeletal muscle (Fig. 8*A*). In addition, it was recently reported that PPARα agonists, such as Wy-14,643, directly enhance lipolysis in isolated adipocytes (41). Thus, it is possible that high concentrations of a PPARα agonist can directly activate PPARα in adipocytes. It remains to be determined which tissue mainly contributes to the improvement in insulin resistance by PPARα activation. To clarify this point, it is necessary to investigate the effects of PPARα agonists in PPARα tissue–specific knockout mice.

It was recently reported that a PPARα/γ agonist elevated pyruvate dehydrogenase kinase isozyme 4 (PDK4) mRNA levels in liver compared with vehicle or a PPARγ agonist (42). In the present study, we checked PDK4 mRNA levels in liver and epididymal adipose tissue and found that PDK4 mRNA levels in epididymal adipose tissue of Wy-14,643–treated KKAy mice were significantly higher than those of vehicle-treated KKAy mice (data not shown), indicating that PPARα was actually activated in adipose tissue by Wy-14,643 treatment. However, there was no significant change in the PDK4 mRNA level in liver between vehicle- and Wy-14,643–treated KKAy mice (data not shown). Precise reasons that explain differences between the results of their study and those of our current study are not known at present. However, several factors, such as animal species (rats and mice), treatment periods (1 and 8 weeks), administration route (oral gavage and mixed chow), and sampling time after the final dose (6 and 24 h) are different between the two studies, which may cause differences in gene expression of PDK4 in liver.

Here we have shown that activation of PPARα suppressed obesity-induced increases in inflammatory cytokines such as TNF-α and MCP-1 in WAT. To the best of our knowledge, this is the first report indicating that the activation of PPARα regulates inflammation in WAT, whereas it has been reported that TZDs also suppressed the increased expression of inflammatory genes in WAT of *ob/ob* mice (14). In the current study, the efficacy of the PPARα agonist appeared to be more potent than that of the PPARγ agonist with respect to suppression of the increased expression of inflammatory molecules in vivo. Although PPARα agonists have been shown to inhibit a nuclear factor-κB pathway stimulated by proinflammatory substances in smooth muscle cells (43,44), the distinct mechanism by which PPARα agonists suppress the expression of inflammatory cytokines in WAT remains to be clarified. However, in this study, a PPARα agonist directly suppressed the increase in MCP-1 expression by proinflammatory substances in cultured adipocytes or macrophages in vitro. Therefore, it is plausible that PPARα can mediate the reduction of proinflammatory substance–induced increase in MCP-1 expression in both adipocytes and infiltrated macrophages in WAT, leading to a reduction of macrophage accumulation and a reversal of adipocyte dysfunction.

Finally, we found that activation of PPARα increased AdipoR1 and -2 expression in both WAT and BAT in vivo. In contrast, activation of PPARα increased only AdipoR2 in cultured cells. This result is consistent with previous studies that found PPARα agonists increased only AdipoR2 expression in cultured macrophages (45). Furthermore, the expression of AdipoR1 and -2 in the liver from Wy-14,643–treated KKAy mice were not significantly changed compared with those from vehicle-treated mice

(data not shown). Therefore, cofactors that are expressed in adipocytes and macrophages and bind with PPARα may be involved in the regulation of AdipoR2 expression. Activation of PPARγ also increased the expression of AdipoR2 in adipocytes in vitro and in vivo, but it did not affect the expression of AdipoR2 in either WAT or BAT in vivo because an increase of AdipoR2 expression in stromal-vascular cells in adipose tissues was not observed after PPARγ activation. The increase of AdipoR2 expression in adipocytes may be caused by the secondary effect on adipocyte differentiation by PPARγ activation because AdipoR2 expression was dramatically increased during adipocyte differentiation (T.Y., T.K., unpublished data). It was recently reported that adiponectin inhibits lipopolysaccharide-induced inflammatory responses in adipocytes (46). Therefore, the increase of AdipoR expression by PPARα activation in adipocytes may enhance adiponectin's anti-inflammatory action in WAT. To date, however, there are no data indicating to what extent increases in AdipoR1 and -2 expression contribute to the improvement in insulin resistance by PPARα activation. Further studies using AdipoR knockout mice will be required to clarify this point. We also showed that activation of PPARγ or food restriction increased the ratio of HMW to total adiponectin and that activation of PPARα did not affect the ratio. This result indicates that an improvement in adipocyte hypertrophy or a reduction in body weight was sufficient to increase the ratio of HMW to total adiponectin. Further investigations will be important to clarify how PPARγ agonists increase HMW adiponectin because HMW adiponectin may be the active form of this protein with respect to its glucose-lowering effect (35) and in the activation of AMP kinase (T.Y., T.K., unpublished data).

In conclusion, as shown in Fig. 9, we have proposed novel mechanisms by which the activation of PPARα and -γ can improve obesity-induced insulin resistance. First, activation of PPARα suppresses inflammation and adipose hypertrophy in WAT. Second, dual activation of PPARα and -γ enhances the action of adiponectin by increasing AdipoR expression and the ratio of HMW to total adiponectin.

ACKNOWLEDGMENTS

This work was supported by the Program for Promotion of Fundamental Studies in Health Sciences of the Organization for Pharmaceutical Safety and Research of Japan; a grant from the Human Science Foundation (to T.K.); a grant-in-aid for the development of innovative technology from the Ministry of Education, Culture, Sports, Science and Technology of Japan (to T.K.); Grant-in Aid for Creative Scientific Research 10NP0201 from the Japan Society for the Promotion of Science (to T.K.); and health science research grants (research on human genome and gene therapy) from the Ministry of Health, Labor and Welfare of Japan (to T.K.).

We are grateful to A. Itoh and A. Okano for their excellent technical assistance.

REFERENCES

1. Kersten S, Desvergne B, Wahli W: Roles of PPARs in health and disease. *Nature* 405:421–424, 2000
2. Lowell BB: PPARγ: an essential regulator of adipogenesis and modulator of fat cell function. *Cell* 99:239–242, 1999
3. Spiegelman BM, Flier JS: Adipogenesis and obesity: rounding out the big picture. *Cell* 87:377–389, 1996
4. Gonzalez FJ: Recent update on the PPAR α-null mouse. *Biochimie* 79:139–144, 1997
5. Auwerx J: PPARγ, the ultimate thrifty gene. *Diabetologia* 42:1033–1049, 1999
6. Evans RM, Barish GD, Wang YX: PPARs and the complex journey to obesity. *Nat Med* 10:355–361, 2004
7. Yamauchi T, Kamon J, Waki H, Murakami K, Motojima K, Komeda K, Ide T, Kubota N, Terauchi Y, Tobe K, Miki H, Tsuchida A, Akanuma Y, Nagai R, Kimura S, Kadowaki T: The mechanisms by which both heterozygous peroxisome proliferator-activated receptor γ (PPARγ) deficiency and PPARγ agonist improve insulin resistance. *J Biol Chem* 276:41245–41254, 2001
8. Yamauchi T, Waki H, Kamon J, Murakami K, Motojima K, Komeda K, Miki H, Kubota N, Terauchi Y, Tsuchida A, Tsuboyama-Kasaoka N, Yamauchi N, Ide T, Hori W, Kato S, Fukayama M, Akanuma Y, Ezaki O, Itai A, Nagai R, Kimura S, Tobe K, Kagechika H, Shudo K, Kadowaki T: Inhibition of RXR and PPARγ ameliorates diet-induced obesity and type 2 diabetes. *J Clin Invest* 108:1001–1013, 2001
9. Yamauchi T, Kamon J, Waki H, Terauchi Y, Kubota N, Hara K, Mori Y, Ide T, Murakami K, Tsuboyama-Kasaoka N, Ezaki O, Akanuma Y, Gavrilova O, Vinson C, Reitman ML, Kagechika H, Shudo K, Yoda M, Nakano Y, Tobe K, Nagai R, Kimura S, Tomita M, Froguel P, Kadowaki T: The fat-derived hormone adiponectin reverses insulin resistance associated with both lipoatrophy and obesity. *Nat Med* 7:941–946, 2001
10. Guerre-Millo M, Gervois P, Raspe E, Madsen L, Poulain P, Derudas B, Herbert JM, Winegar DA, Willson TM, Fruchart JC, Berge RK, Staels B: Peroxisome proliferator-activated receptor α activators improve insulin sensitivity and reduce adiposity. *J Biol Chem* 275:6638–16642, 2000
11. Ye JM, Doyle PJ, Iglesias MA, Watson DG, Cooney GJ, Kraegen EW: Peroxisome proliferator-activated receptor (PPAR)-α activation lowers muscle lipids and improves insulin sensitivity in high fat-fed rats: comparison with PPAR-γ activation. *Diabetes* 50:411–417, 2001
12. Chou CJ, Haluzik M, Gregory C, Dietz KR, Vinson C, Gavrilova O, Reitman ML: WY14,643, a peroxisome proliferator-activated receptor alpha (PPARα) agonist, improves hepatic and muscle steatosis and reverses insulin resistance in lipoatrophic A-ZIP/F-1 mice. *J Biol Chem* 277:24484–24489, 2002
13. Weisberg SP, McCann D, Desai M, Rosenbaum M, Leibel RL, Ferrante AW Jr: Obesity is associated with macrophage accumulation in adipose tissue. *J Clin Invest* 112:1796–1808, 2003
14. Xu H, Barnes GT, Yang Q, Tan G, Yang D, Chou CJ, Sole J, Nichols A, Ross JS, Tartaglia LA, Chen H: Chronic inflammation in fat plays a crucial role in the development of obesity-related insulin resistance. *J Clin Invest* 112:1821–1830, 2003
15. Pickup JC, Mattock MB, Chusney GD, Burt D: NIDDM as a disease of the innate immune system: association of acute-phase reactants and interleukin-6 with metabolic syndrome X. *Diabetologia* 40:1286–1292, 1997
16. Yudkin JS, Stehouwer CD, Emeis JJ, Coppack SW: C-reactive protein in healthy subjects: associations with obesity, insulin resistance, and endothelial dysfunction: a potential role for cytokines originating from adipose tissue? *Arterioscler Thromb Vasc Biol* 19:972–978, 1999
17. Festa A, D'Agostino R Jr, Howard G, Mykkanen L, Tracy RP, Haffner SM: Chronic subclinical inflammation as part of the insulin resistance syndrome: the Insulin Resistance Atherosclerosis Study (IRAS). *Circulation* 102:42–47, 2000
18. Lehmann JM, Kliewer SA, Moore LB, Smith-Oliver TA, Oliver BB, Su JL, Sundseth SS, Winegar DA, Blanchard DE, Spencer TA, Willson TM: Activation of the nuclear receptor LXR by oxysterols defines a new hormone response pathway. *J Biol Chem* 270:12953–12956, 1995
19. Yamauchi T, Kamon J, Ito Y, Tsuchida A, Yokomizo T, Kita S, Sugiyama T, Miyagishi M, Hara K, Tsunoda M, Murakami K, Ohteki T, Uchida S, Takekawa S, Waki H, Tsuno NH, Shibata Y, Terauchi Y, Froguel P, Tobe K, Koyasu S, Taira K, Kitamura T, Shimizu T, Nagai R, Kadowaki T: Cloning of adiponectin receptors that mediate antidiabetic metabolic effects. *Nature* 423:762–769, 2003
20. Kubota N, Terauchi Y, Yamauchi T, Kubota T, Moroi M, Matsui J, Eto K, Yamashita T, Kamon J, Satoh H, Yano W, Froguel P, Nagai R, Kimura S, Kadowaki T, Noda T: Disruption of adiponectin causes insulin resistance and neointimal formation. *J Biol Chem* 277:25863–25866, 2002
21. Motojima K, Passilly P, Peters JM, Gonzalez FJ, Latruffe N: Expression of putative fatty acid transporter genes are regulated by peroxisome proliferator-activated receptor α and γ activators in a tissue- and inducer-specific manner. *J Biol Chem* 273:16710–16714, 1998
22. Chao L, Marcus-Samuels B, Mason MM, Moitra J, Vinson C, Arioglu E, Gavrilova O, Reitman ML: Adipose tissue is required for the antidiabetic, but not for the hypolipidemic, effect of thiazolidinediones. *J Clin Invest* 106:1221–1228, 2000
23. Moore GB, Chapman H, Holder JC, Lister CA, Piercy V, Smith SA, Clapham

JC: Differential regulation of adipocytokine mRNAs by rosiglitazone in db/db mice. *Biochem Biophys Res Commun* 286:735–741, 2001
24. Kim H, Haluzik M, Asghar Z, Yau D, Joseph JW, Fernandez AM, Reitman ML, Yakar S, Stannard B, Heron-Milhavet L, Wheeler MB, LeRoith D: Peroxisome proliferator–activated receptor-α agonist treatment in a transgenic model of type 2 diabetes reverses the lipotoxic state and improves glucose homeostasis. *Diabetes* 52:1770–1778, 2003
25. Waki H, Yamauchi T, Kamon J, Ito Y, Uchida S, Kita S, Hara K, Hada Y, Vasseur F, Froguel P, Kimura S, Nagai R, Kadowaki T: Impaired multimerization of human adiponectin mutants associated with diabetes: molecular structure and multimer formation of adiponectin. *J Biol Chem* 278:40352–40363, 2003
26. Li AC, Binder CJ, Gutierrez A, Brown KK, Plotkin CR, Pattison JW, Valledor AF, Davis RA, Willson TM, Witztum JL, Palinski W, Glass CK: Differential inhibition of macrophage foam-cell formation and atherosclerosis in mice by PPARα, β/δ, and γ. *J Clin Invest* 114:1564–1576, 2004
27. Barbera MJ, Schluter A, Pedraza N, Iglesias R, Villarroya F, Giralt M: Peroxisome proliferator-activated receptor α activates transcription of the brown fat uncoupling protein-1 gene: a link between regulation of the thermogenic and lipid oxidation pathways in the brown fat cell. *J Biol Chem* 276:1486–1493, 2001
28. Fu J, Gaetani S, Oveisi F, Lo Verme J, Serrano A, Rodriguez De Fonseca F, Rosengarth A, Luecke H, Di Giacomo B, Tarzia G, Piomelli D: Oleylethanolamide regulates feeding and body weight through activation of the nuclear receptor PPAR-α. *Nature* 425:90–93, 2003
29. Braissant O, Foufelle F, Scotto C, Dauca M, Wahli W: Differential expression of peroxisome proliferator-activated receptors (PPARs): tissue distribution of PPAR-α, -β, and -γ in the adult rat. *Endocrinology* 137:354–366, 1996
30. Auboeuf D, Rieusset J, Fajas L, Vallier P, Frering V, Riou JP, Staels B, Auwerx J, Laville M, Vidal H: Tissue distribution and quantification of the expression of mRNAs of peroxisome proliferator-activated receptors and liver X receptor-α in humans: no alteration in adipose tissue of obese and NIDDM patients. *Diabetes* 46:1319–1327, 1997
31. Sartipy P, Loskutoff DJ: Monocyte chemoattractant protein 1 in obesity and insulin resistance. *Proc Natl Acad Sci U S A* 100:7265–7270, 2003
32. Tsuchida A, Yamauchi T, Ito Y, Hada Y, Maki T, Takekawa S, Kamon J, Kobayashi M, Suzuki R, Hara K, Kubota N, Terauchi Y, Froguel P, Nakae J, Kasuga M, Accili D, Tobe K, Ueki K, Nagai R, Kadowaki T: Insulin/Foxo1 pathway regulates expression levels of adiponectin receptors and adiponectin sensitivity. *J Biol Chem* 279:30817–30822, 2004
33. Crouch E, Persson A, Chang D, Heuser J: Molecular structure of pulmonary surfactant protein D (SP-D). *J Biol Chem* 269:17311–17319, 1994
34. McCormack FX, Pattanajitvilai S, Stewart J, Possmayer F, Inchley K, Voelker DR: The Cys6 intermolecular disulfide bond and the collagen-like region of rat SP-A play critical roles in interactions with alveolar type II cells and surfactant lipids. *J Biol Chem* 272:27971–27979, 1997
35. Pajvani UB, Hawkins M, Combs TP, Rajala MW, Doebber T, Berger JP, Wagner JA, Wu M, Knopps A, Xiang AH, Utzschneider KM, Kahn SE, Olefsky JM, Buchanan TA, Scherer PE: Complex distribution, not absolute amount of adiponectin, correlates with thiazolidinedione-mediated improvement in insulin sensitivity. *J Biol Chem* 279:12152–12162, 2004
36. Flier JS: Obesity wars: molecular progress confronts an expanding epidemic. *Cell* 116:337–350, 2004
37. Kelly LJ, Vicario PP, Thompson GM, Candelore MR, Doebber TW, Ventre J, Wu MS, Meurer R, Forrest MJ, Conner MW, Cascieri MA, Moller DE: Peroxisome proliferator-activated receptors γ and α mediate in vivo regulation of uncoupling protein (UCP-1, UCP-2, UCP-3) gene expression. *Endocrinology* 139:4920–4927, 1998
38. Armstrong MB, Towle HC: Polyunsaturated fatty acids stimulate hepatic UCP-2 expression via a PPARα-mediated pathway. *Am J Physiol* 281: E1197–E1204, 2001
39. Granneman JG, Lahners KN, Chaudhry A: Molecular cloning and expression of the rat β3-adrenergic receptor. *Mol Pharmacol* 40:895–899, 1991
40. Atgie C, D'Allaire F, Bukowiecki LJ: Role of β1- and β3-adrenoceptors in the regulation of lipolysis and thermogenesis in rat brown adipocytes. *Am J Physiol* 273:C1136–C1142, 1997
41. Guzman M, Lo Verme J, Fu J, Oveisi F, Blazquez C, Piomelli D: Oleoylethanolamide stimulates lipolysis by activating the nuclear receptor peroxisome proliferator-activated receptor α (PPAR-α). *J Biol Chem* 279:27849–27854, 2004
42. Reifel-Miller A, Otto K, Hawkins E, Barr R, Bensch WR, Bull C, Dana S, Klausing K, Martin JA, Rafaeloff-Phail R, Rafizadeh-Montrose C, Rhodes G, Robey R, Rojo I, Rungta D, Snyder D, Wilbur K, Zhang T, Zink R, Warshawsky A, Brozinick JT: A peroxisome proliferator-activated receptor α/γ dual agonist with a unique in vitro profile and potent glucose and lipid effects in rodent models of type 2 diabetes and dyslipidemia. *Mol Endocrinol* 19:1593–1605, 2005
43. Staels B, Koenig W, Habib A, Merval R, Lebret M, Torra IP, Delerive P, Fadel A, Chinetti G, Fruchart JC, Najib J, Maclouf J, Tedgui A: Activation of human aortic smooth-muscle cells is inhibited by PPARα but not by PPARγ activators. *Nature* 393:790–793, 1998
44. Delerive P, De Bosscher K, Besnard S, Vanden Berghe W, Peters JM, Gonzalez FJ, Fruchart JC, Tedgui A, Haegeman G, Staels B: Peroxisome proliferator-activated receptor α negatively regulates the vascular inflammatory gene response by negative cross-talk with transcription factors NF-κB and AP-1. *J Biol Chem* 274:32048–54, 1999
45. Chinetti G, Zawadski C, Fruchart JC, Staels B: Expression of adiponectin receptors in human macrophages and regulation by agonists of the nuclear receptors PPARα, PPARγ, and LXR. *Biochem Biophys Res Commun* 314:151–158, 2004
46. Ajuwon KM, Spurlock ME: Adiponectin inhibits lipopolysaccharide-induced NF-κB activation and IL-6 production and increases PPARγ2 expression in adipocytes. *Am J Physiol Regul Integr Comp Physiol* 288:R1220–R1225, 2005

Diabetologia (2005) 48: 1307–1314
DOI 10.1007/s00125-005-1806-3

ARTICLE

K. Hara · M. Horikoshi · H. Kitazato · T. Yamauchi · C. Ito · M. Noda · J. Ohashi · P. Froguel · K. Tokunaga · R. Nagai · T. Kadowaki

Absence of an association between the polymorphisms in the genes encoding adiponectin receptors and type 2 diabetes

Received: 8 November 2004 / Accepted: 5 April 2005 / Published online: 26 May 2005

Abstract *Aims/hypothesis:* Secreted by adipocytes, adiponectin is a hormone that acts as an antidiabetic and anti-atherogenic adipokine. We recently cloned the genes encoding two adiponectin receptors (*ADIPOR1* and *ADIPOR2*). The aim of this study was to examine whether *ADIPOR1* and/or *ADIPOR2* play a major role in genetic susceptibility to insulin resistance or type 2 diabetes in the Japanese population. *Methods:* By direct sequencing and a search of public databases, we identified single nucleotide polymorphisms (SNPs) in *ADIPOR1* and *ADIPOR2*, and investigated whether these SNPs are associated with insulin resistance and type 2 diabetes in the Japanese population. *Results:* The linkage disequilibrium (LD) in the chromosomal region of *ADIPOR1* was almost completely preserved, whereas the LD in *ADIPOR2* was less well preserved. None of the SNPs in *ADIPOR1* or *ADIPOR2* were significantly associated with insulin resistance or type 2 diabetes. No differences in *ADIPOR1* or *ADIPOR2* haplotype frequencies were observed between type 2 diabetic and non-diabetic subjects. *Conclusions/interpretation:* Genetic variations in *ADIPOR1* or *ADIPOR2* are unlikely to lead to a common genetic predisposition to insulin resistance or type 2 diabetes in the Japanese population.

Keywords Association · Polymorphism · Susceptibility gene

Abbreviations LD: linkage disequilibrium · ESM: electronic supplementary material · HOMA: homeostasis model assessment · SNP: single nucleotide polymorphism

Introduction

Adiponectin (also known as the 30-kDa adipocyte complement-related protein, or Acrp30) [1–4] is a hormone secret-

Electronic supplementary material Supplementary material is available for this article at http://dx.doi.org/10.1007/s00125-005-1806-3.

K. Hara · M. Horikoshi · T. Yamauchi · T. Kadowaki (✉)
Department of Metabolic Diseases,
Graduate School of Medicine, University of Tokyo,
7-3-1 Hongo, Bunkyo-ku,
Tokyo, 113-8655, Japan
e-mail: kadawaki-3im@h.u-tokyo.ac.jp
Tel.: +81-35-8008815
Fax: +81-35-8009797

K. Hara · R. Nagai
Department of Clinical Bioinformatics,
Graduate School of Medicine, University of Tokyo,
Tokyo, Japan

K. Hara · T. Kadowaki
Core Research for Evolution Science and Technology (CREST),
Japan Science and Technology Corporation (JST),
Tokyo, Japan

H. Kitazato
Institute for Diabetes Care and Research,
Asahi Life Foundation,
Tokyo, Japan

C. Ito
Hiroshima Atomic Bomb Casualty Council Health
Management Center,
Hiroshima, Japan

M. Noda
Department of Endocrinology and Metabolism,
Toranomon Hospital,
Tokyo, Japan

J. Ohashi · K. Tokunaga
Department of Human Genetics,
Graduate School of Medicine, University of Tokyo,
Tokyo, Japan

P. Froguel
Institute of Biology—CNRS 8090,
Pasteur Institute of Lille,
Lille, France

P. Froguel
Imperial College Genome Centre and Genomic Medicine,
London, UK

ed by adipocytes that acts as an antidiabetic adipokine [5–9]. Levels of adiponectin in the blood are decreased in subjects with obesity, insulin resistance or type 2 diabetes [10, 11]. In animal models, decreased plasma adiponectin is causally involved in insulin resistance and glucose intolerance [6–9]. In humans, polymorphisms in the gene encoding adiponectin have been shown to be associated with insulin resistance and type 2 diabetes [12–14].

We recently cloned cDNAs encoding adiponectin receptors 1 and 2 (*ADIPOR1* and *ADIPOR2*) [15]. These receptors mediate increases in the AMP kinase [16] and peroxisome proliferator-activated receptor-α ligand activities [17] of adiponectin [15], and are likely to mediate the insulin-sensitising actions of adiponectin. Therefore, *ADIPOR1* and *ADIPOR2* may be viewed as plausible candidate genes for susceptibility to insulin resistance and type 2 diabetes.

The aim of this study was to investigate whether single nucleotide polymorphisms (SNPs) in *ADIPOR1* and *ADIPOR2* influence insulin resistance and susceptibility to type 2 diabetes in the Japanese population.

Subjects and methods

Subjects The inclusion criteria for the diabetic and non-diabetic subjects enrolled in this study have been described previously [13]. Diabetes was diagnosed according to the criteria of the World Health Organization [18]. All subjects enrolled in this study were of full Japanese ancestry. SNPs in *ADIPOR1* and *ADIPOR2* were genotyped in 192 diabetic and 192 non-diabetic subjects. The clinical characteristics of the subjects are described in Table 1 of the electronic supplementary material (ESM). Written informed consent was obtained from the subjects, and the study was approved by the Ethics Committee of the University of Tokyo.

Biological measurements Insulin resistance and beta cell function were assessed using homeostasis model assessment (HOMA). The HOMA of insulin resistance (HOMA-IR) was calculated as fasting insulin (μU/ml)×glucose (mmol/l)/22.5, as described elsewhere [19]. Data are expressed as means±SEM. Since the use of insulin therapy or oral hypoglycaemic agents in subjects with type 2 diabetes is likely to interfere with insulin levels, the correlations between SNPs and insulin resistance were only assessed in non-diabetic subjects.

Screening and selection of SNPs in ADIPOR1 and ADIPOR2 To establish an SNP map encompassing *ADIPOR1* and *ADIPOR2*, SNPs were identified by direct sequencing and a search of public databases. All eight exons in *ADIPOR1* and all nine exons in *ADIPOR2*, plus 50–100 bases of the 5′ and 3′ intronic regions flanking the exons, were amplified and directly sequenced in 30 type 2 diabetic subjects. The conditions and the sequences of the primers used

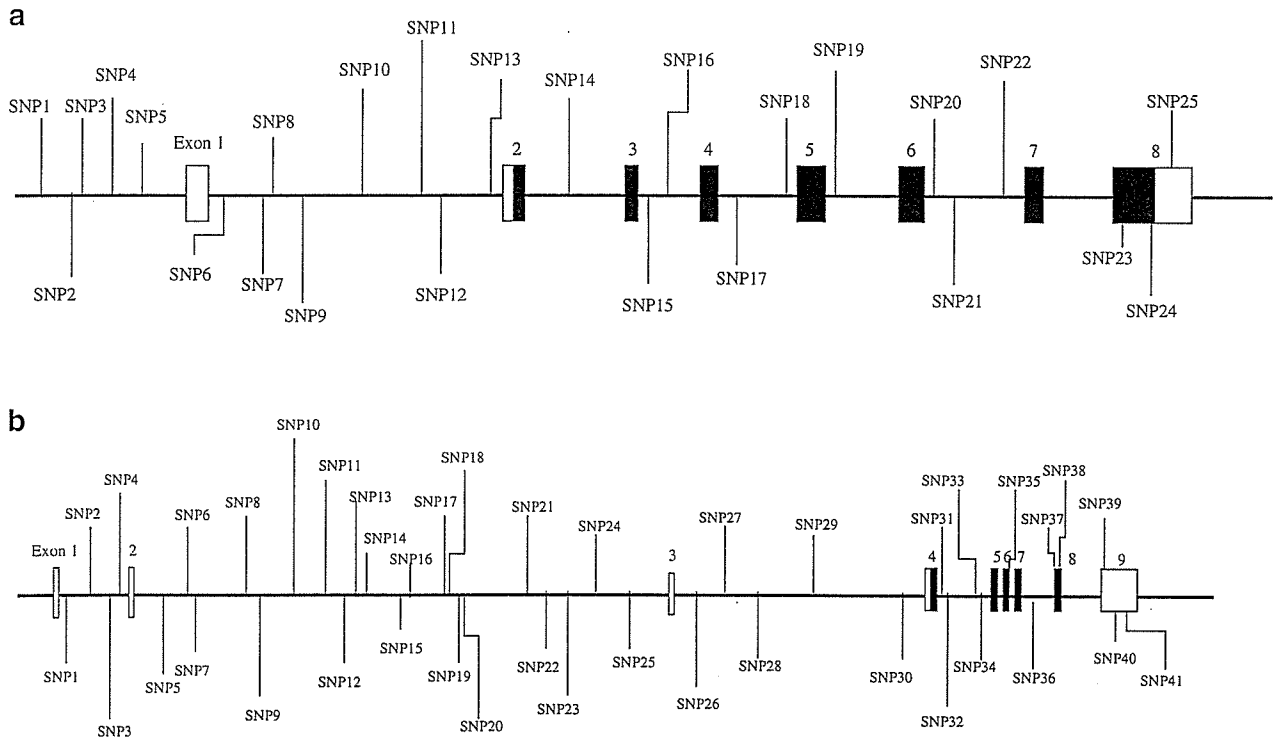

Fig. 1 Genomic structure of *ADIPOR1* (**a**) and *ADIPOR2* (**b**) and the locations of the SNPs genotyped in the present study. Exons are shown as *boxes*, and introns and flanking sequences as *lines connecting the boxes*. Coding sequences are represented as *closed boxes*, and untranslated regions as *open boxes*. The SNPs are numbered in order of appearance from the 5′ to 3′ ends of the genes

in the PCR are described in Table 2 of the ESM. The SNPs were identified based on the sequences reported in the GenBank database (http://www.ncbi.nih.gov/index.html), which contains *ADIPOR1* (accession number NT_004671) and *ADIPOR2* (accession number NT_009759). From the public database, 14 SNPs in *ADIPOR1* (rs6666089, rs109 20534, rs12039275, rs12733285, rs1539355, rs2275738, rs2275737, rs2275735, rs1342387, rs3737884, rs2275736, rs11581, rs1043268, rs1043280) and 29 SNPs in *ADI POR2* (rs2058033, rs6489322, rs12579507, rs11061935, rs7975600, rs10773982, rs11829703, rs12810020, rs110 61947, rs11612383, rs11612726, rs9888418, rs7976827, rs12582624, rs10848566, rs7297509, rs12818963, rs108 48569, rs11061974, rs2068485, rs7974924, rs12831353, rs12828908, rs10848571, rs7974422, rs2286385, rs730 032, rs12342, rs1044471) were selected and validated in 30 type 2 diabetic subjects. From the database, we chose SNPs with a minor allele frequency higher than 10%; we excluded those SNPs for which information on allele frequency was not presented. In total, 25 SNPs in *ADIPOR1* and 41 SNPs in *ADIPOR2* were identified. Minor allele frequency was determined and Hardy–Weinberg equilibrium was assessed. We eliminated SNPs that deviated from Hardy–Weinberg equilibrium or that had a minor allele frequency lower than 10% from further study. In total, 14 SNPs in *ADIPOR1* and 24 SNPs in *ADIPOR2* were analysed, resulting in an average SNP density of one SNP per 1.2 kb in *ADIPOR1* and one SNP per 3.9 kb in *ADIPOR2*.

Genotyping of SNPs used in the association study We genotyped the SNPs in *ADIPOR1* and *ADIPOR2* in type 2 diabetic subjects and non-diabetic subjects using direct sequencing. PCR was performed under standard conditions. Sequencing reactions were performed using the Big Dye terminator kit (Applied Biosystems, Foster City, CA, USA), and the products were resolved using an ABI 3700 automated DNA sequencer (Applied Biosystems). The results were integrated using a Sequencher (Gene Codes Corporation, Ann Arbor, MI, USA), and individual SNPs were manually genotyped. Ambiguous base assignments were eliminated from further analysis.

Statistical analysis The proportions of genotypes or alleles between subjects with or without type 2 diabetes were compared using a chi square (χ^2) test. The differences between subjects with different SNP genotypes were statistically tested using an ANOVA. A Bonferroni adjustment was used to avoid type 1 errors caused by multiple testing. The level of significance for SNPs in *ADIPOR1* and *ADIPOR2* was 0.001 (0.05 divided by 38, the total number

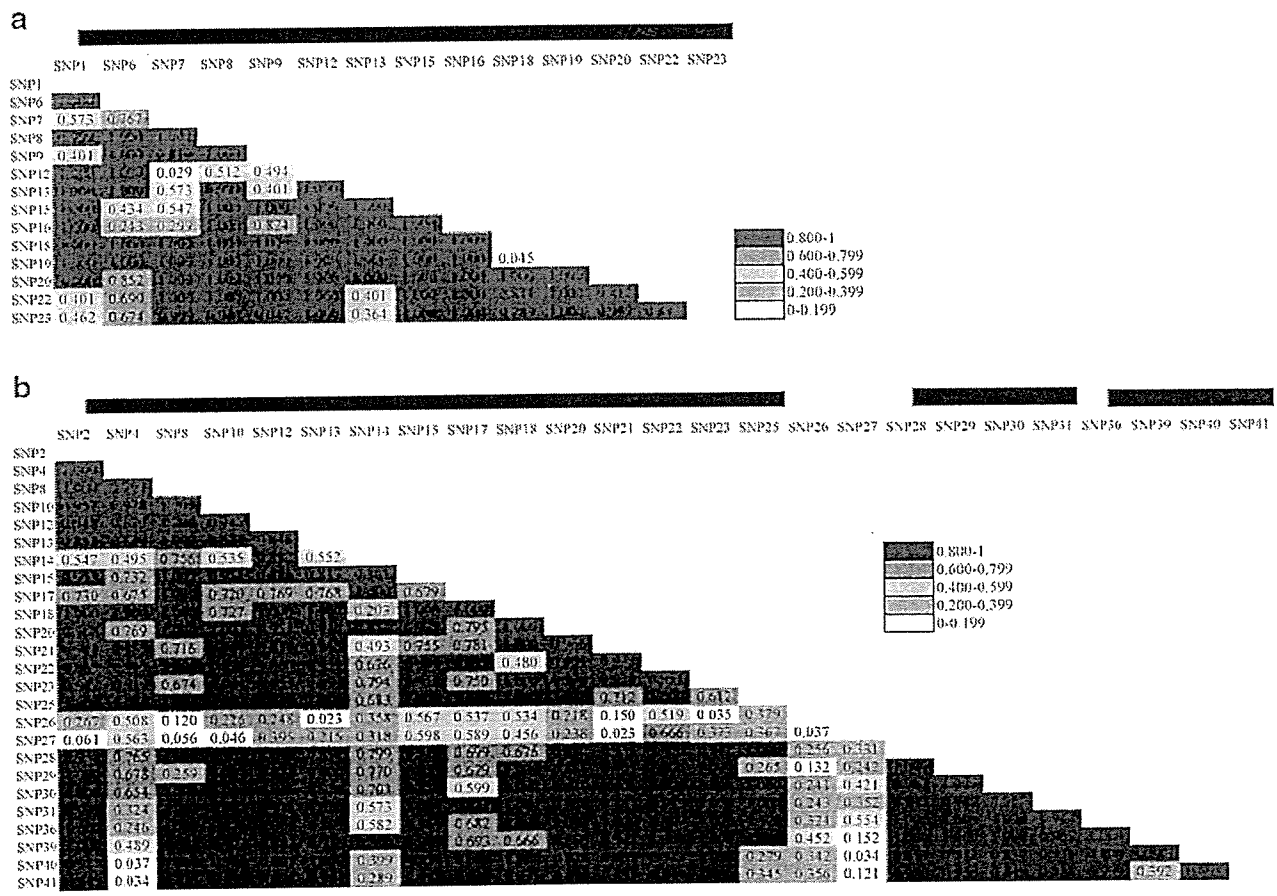

Fig. 2 The pairwise marker LD between SNPs in *ADIPOR1* (a) and *ADIPOR2* (b). The LD between a pair of markers is indicated by the colour of the block (*blue to red*). Block structure is indicated at the top of each figure as a *closed box*